ELECTRIC POWER
RESEARCH INSTITUTE

Evaluation of the Impact of Neutron Absorber Material Blistering and Pitting on Spent Fuel Pool Reactivity

2018 TECHNICAL REPORT

Evaluation of the Impact of Neutron Absorber Material Blistering and Pitting on Spent Fuel Pool Reactivity

All or a portion of the requirements of the EPRI Nuclear Quality Assurance Program apply to this product.

YES NO

EPRI Project Manager
H. Akkurt

ELECTRIC POWER RESEARCH INSTITUTE

3420 Hillview Avenue
Palo Alto, CA 94304-1338
USA

PO Box 10412
Palo Alto, CA 94303-0813
USA

800.313.3774
650.855.2121

askepri@epri.com

www.epri.com

3002013119
Final Report, May 2018

THE FOLLOWING ORGANIZATIONS PREPARED THIS REPORT:

Electric Power Research Institute (EPRI)

Westinghouse Electric Company

THE TECHNICAL CONTENTS OF THIS PRODUCT WERE **NOT** PREPARED IN ACCORDANCE WITH THE EPRI QUALITY PROGRAM MANUAL THAT FULFILLS THE REQUIREMENTS OF 10 CFR 50, APPENDIX B. THIS PRODUCT IS **NOT** SUBJECT TO THE REQUIREMENTS OF 10 CFR PART 21.

NOTE

For further information about EPRI, call the EPRI Customer Assistance Center at 800.313.3774 or e-mail askepri@epri.com.

Acknowledgments

The following organizations prepared this report.

The Electric Power Research Institute

Principal Investigator
H. Akkurt

Westinghouse Electric Company
Cranberry Woods Headquarters
1000 Westinghouse Drive
Cranberry Township, PA 16066

Principal Investigators
M. Wenner
A. Blanco

This report describes research sponsored by EPRI.

This publication is a corporate document that should be cited in the literature in the following manner:

Evaluation of the Impact of Neutron Absorber Material Blistering and Pitting on Spent Fuel Pool Reactivity. EPRI, Palo Alto, CA: 2018. 3002013119.

Abstract

Neutron absorber materials are used in spent fuel pool (SFP) storage racks to increase storage capacity while maintaining criticality safety margins. Operating experience to date has revealed blistering and pitting in BORAL®, a commonly used neutron absorber material in SFPs in the U.S. and many other countries. The objective of this study is to generically evaluate the impact of blisters and pits on SFP reactivity. For broader applicability, simulations were performed for a generic neutron absorber material, which has no protective cladding such that the results can be applicable not only for BORAL® but for other metal matrix composite neutron absorber materials that are used in SFPs. Since BORAL® has the longest history, operating experience to date for BORAL® has been evaluated, and the worst cases, in terms of pit and blister sizes, have been simulated. This part of the analysis demonstrated that even in the worst operating experience case, the impact on reactivity is insignificant (<100 pcm). Then, hypothetical extreme cases were evaluated to determine bounds for future operation. Analysis was performed for two fuel types used in Pressurized Water Reactors (PWR) to determine the impact of different fuel types. Simulations were performed at unborated conditions such that the results could be applicable for neutron absorber materials used in Boiling Water Reactors (BWR) SFPs or SFPs that do not contain boron. This report presents the approach for the evaluation and the computational results.

Keywords
Neutron absorber material
Spent fuel pool
Criticality
Blister and pit

ELECTRIC POWER RESEARCH INSTITUTE

Deliverable Number: 3002013119

Product Type: Technical Report

Product Title: Evaluation of the Impact of Neutron Absorber Material Blistering and Pitting on Spent Fuel Pool Reactivity

---

PRIMARY AUDIENCE: Neutron absorber material users for spent fuel wet storage applications

SECONDARY AUDIENCE: Neutron absorber material users in general, including regulators and vendors, for wet storage applications

KEY RESEARCH QUESTION

Operating experience has shown that over time, metal matrix neutron absorber materials containing B_4C and aluminum develop pitting, and those absorbers that have aluminum cladding might also develop blistering. Given the observed blistering and pitting, the key research questions are:

- Is the observed blistering and pitting at a level that could cause potential concern for criticality safety of the spent fuel pools (SFP)?
- What are the conditions and limits when blisters and/or pits start to show an impact on SFP criticality?

RESEARCH OVERVIEW

To address these questions, several thousands of simulations were performed. The computations were performed using Scale 6.1 with 238 group ENDF/B-VII cross section libraries. To answer these questions as generically as possible for a wide range of neutron absorber materials containing boron carbide and aluminum as a metal matrix composite, in the simulations, it is assumed that the neutron absorber material does not have cladding for the pitting analysis.

KEY FINDINGS

- The blistering and pitting phenomena observed to date, based on operating experience, have negligible impact on the results and conclusions of SFP criticality safety analyses.
- Significantly larger pit and blister sizes, compared to operating experience, are needed to observe any statistically significant impact on reactivity.
- The results and conclusions presented in this report are applicable to wet storage environments using metal matrix material containing B_4C and aluminum for both pressurized water reactor (PWR) and boiling water reactor (BWR) SFPs.

WHY THIS MATTERS

Based on the analysis performed, the blistering and pitting observed to date on the metallic neutron absorber materials containing B_4C and Al will not have a statistically significant impact on SFP reactivity that would require reevaluation of the SFP criticality analysis. Blister and pit sizes would need to be orders of magnitude larger than presently observed to result in statistically significant impacts to reactivity. Continued monitoring and participation in the industrywide monitoring program is recommended to ensure safety margins are maintained.

HOW TO APPLY RESULTS

The computational results showed that the degradation observed to date from operating experience has negligible impact on SFP reactivity. The results are applicable to both PWRs and BWRs. Although the results show that the degradation to date has negligible impact on reactivity, EPRI recommends that the industry collectively continue to monitor for any trends, outliers, or sudden changes as well as continue to monitor the neutron absorber materials via coupon analysis, and contribute to EPRI's SFP water chemistry and coupon databases.

LEARNING AND ENGAGEMENT OPPORTUNITIES

- The Electric Power Research Institute (EPRI) initiated the SFP water chemistry and coupon databases to continue monitoring conditions and identify any trends for long term performance. Participation in the industrywide learning aging management program (i-LAMP) for neutron absorber materials in SFPs is recommended.
- EPRI's Neutron Absorber User Group (NAUG) is an annual meeting hosted by EPRI, and attendance is generally limited to utility members. NAUG is a platform for exchanging operating experience and determining research needs.

EPRI CONTACTS: Hatice Akkurt, Principal Technical Leader, hakkurt@epri.com

PROGRAM: Used Fuel and High-Level Waste Management Program, Program 41.03.01

IMPLEMENTATION CATEGORY: Reference

Acronyms

BONAMI	Bondarenko AMPX Interpolator
BWR	Boiling Water Reactor
CENTRM	Continuous Energy Transport Module
EPRI	Electric Power Research Institute
GT	Guide Tube
GWd/MTU	Gigawatt-days per metric ton uranium
IFBA	Integral Fuel Burnable Absorber
IT	Instrument Tube
k_{eff}	effective neutron multiplication factor
MMC	Metal Matrix Composite
NAM	Neutron Absorber Material
NAUG	Neutron Absorber User Group
NRC	Nuclear Regulatory Commission
PMC	Produce Multigroup Cross sections
ppm	parts per million
PWR	Pressurized Water Reactor
SFP	Spent Fuel Pool
WABA	Wet Annular Burnable Absorber

Table of Contents

List of Figures

List of Tables

Section 1: Introduction

In spent fuel pools (SFPs), neutron absorber panels are used to increase storage capacity while maintaining criticality safety margins. Earlier neutron absorber materials based on polymers, like Boraflex, have shown significant degradation when exposed to gamma radiation in SFP environments [1]. The majority of the SFPs that used Boraflex in the past either replaced it or reevaluated with the removal of the credit for the absorber.

The metal matrix composite (MMC) neutron absorber materials (NAMs) include BORAL®, Metamic, Boralcan, Bortec, and MAXUS [2]. Some of these MMCs include aluminum cladding on both sides of the core containing B_4C and aluminum. Examples include BORAL® [1], MAXUS [2], and Bortec [1]. While cladding serves as a protective layer, it also makes the material susceptible to the formation of blisters. This is especially true at high temperatures and depends on the material's vintage and porosity. The other MMCs, like Metamic and Boralcan, do not have cladding; consequently, they are not susceptible to blistering. MMCs are susceptible to pitting corrosion (hereafter, pitting) over time.

BORAL® is a commonly used neutron absorber material in SFPs in the U. S. and many countries, including Mexico, Korea, and Taiwan. The first use of BORAL® was at Yankee Rowe in 1964 [1]. Operating experience to date with BORAL® has shown that despite observed blisters and pits, BORAL® is continuing to perform its intended function in SFPs. This operating experience is documented in two EPRI reports [1, 2] and includes a database of the coupon monitoring results from many spent fuel pools spanning over 20 years [3].

Operating experience has shown that metal matrix neutron absorber materials over time are susceptible to pitting, and those absorbers that have cladding may also develop blistering. Given the observed blistering and pitting, the key research questions include:

- Is the observed blistering and pitting at a level that could cause potential concern for criticality safety of the SFPs?
- What are the conditions and limits when blisters and/or pits start to show an impact on SFP criticality?

To address these questions, EPRI initiated a study focused on the evaluation of the impact of blisters and pits on SFP reactivity. This report presents the parameters of the study and the computational results.

The organization of the report is as follows: Section 2 provides background on NAMs with a review of operating experience to date and EPRI research activities toward understanding the long-term performance of NAMs. The description of the fuel assembly and rack geometries used in this study are presented in Section 3. The modeling and simulation codes used in the analysis and the description of the modeling approach for blisters and pits are presented in Section 4. Pitting and blistering analyses and results are presented in Section 5 and Section 6, respectively. The summary of the results and conclusions are presented in Section 7.

Section 2: Background

Some of the metal matrix neutron absorber materials (for example, BORAL®, Bortec, MAXUS) contain aluminum (Al) cladding on both sides of the core while other materials (for example, Metamic, Boralcan) do not have cladding material. This Al cladding can serve as a protective barrier. The thickness of the Al cladding varies with the material. However, the Al cladding is susceptible to uniform and pitting corrosion. Ingress of water into the core can also result in the formation of blisters between the core material and cladding. The core material, mixture of Al and B_4C, is porous. The Al cladding and the core of the absorber are shown in Figure 2-1 for BORAL® [1].

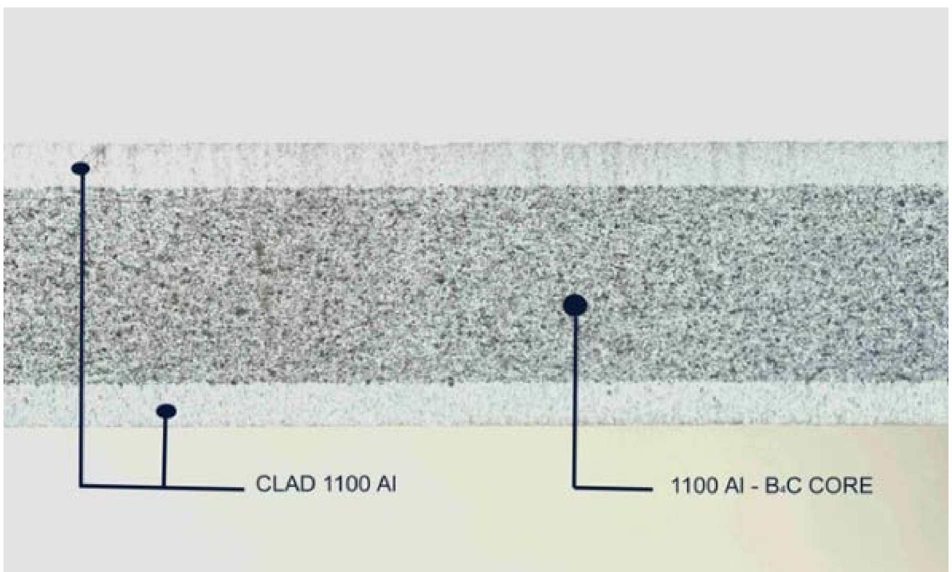

Figure 2-1
Micrograph of BORAL®

Blisters are only expected to be observed for MMCs with Al cladding. One of the MMCs, BORAL®, has been used since 1964 and operating experience with BORAL® has shown that over time blisters and pits (visible primarily via close visual examination and microscopy) are observed. Figure 2-2 shows two BORAL® SFP monitoring coupons, one with multiple blisters (left) [1] and another coupon with a single blister (right) [4].

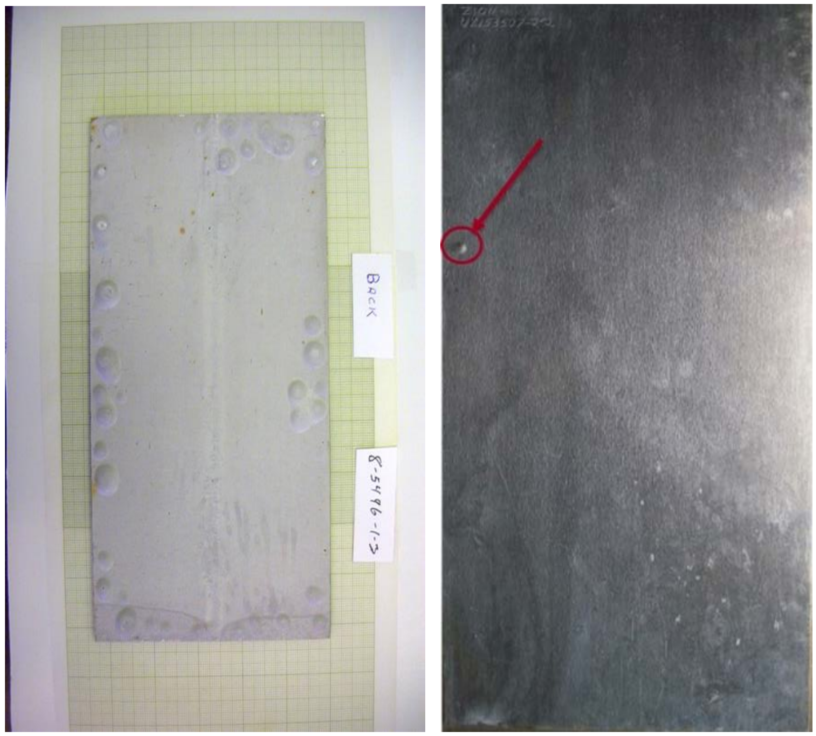

Figure 2-2
BORAL® coupons showing multiple blisters (left) and single blister (right)

Pits can be observed in all types of MMC NAMs, with or without cladding. Figure 2-3 shows a BORAL® coupon with multiple pits that are not yet reached to core (left) and a single pit that breached the cladding and reached to the core (right) [3-4]. It should be noted that these pictures are obtained under a microscope with 100x magnification; hence, not visible to the eye.

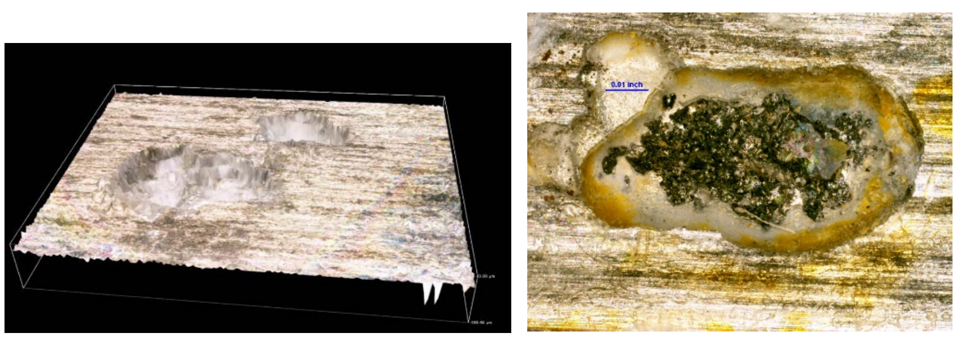

Figure 2-3
BORAL® coupon, under a microscope with 100x magnification, showing multiple pits that have not reached the core (left) and a single pit that has reached the core (right)

2.1 Operating Experience Based on Coupon Data

EPRI published a report in 2010 that summarized operating experience for BORAL® based on the coupon monitoring analysis results. The report includes data from over 100 coupons from over 20 PWR and BWR spent fuel pools. For the coupons included in this study, the service time in the SFP varied from 1 to 16 years for PWR coupons and 5 to 28 years for BWR coupons [3]. None of the coupons showed any statistically significant change in areal density.

The pit depths for over 100 BORAL® coupons, representing coupons from 20 SFPs, are plotted in Figure 2-4. The pit area for the same BORAL® coupons is presented in Figure 2-5. Based on the actual coupon data from SFPs:

- The maximum pit depth is 0.1016 cm (0.04 in.). For BORAL®, the thickness of the Al cladding varies from 10-12 mil (0.025 cm or 0.01 in.) [1]. As shown in the figure, some of the pit depths are below 0.025 cm, which indicates the Al cladding has not been breached.
- The maximum pit area is ~0.3 cm^2 (0.046 in^2). As shown in the figure, the majority of the pit areas are below 0.15 cm^2 and there is only one point where max area is observed.
- The pit with maximum depth and the pit with the maximum area do not correspond to the same pit or even the same coupon.

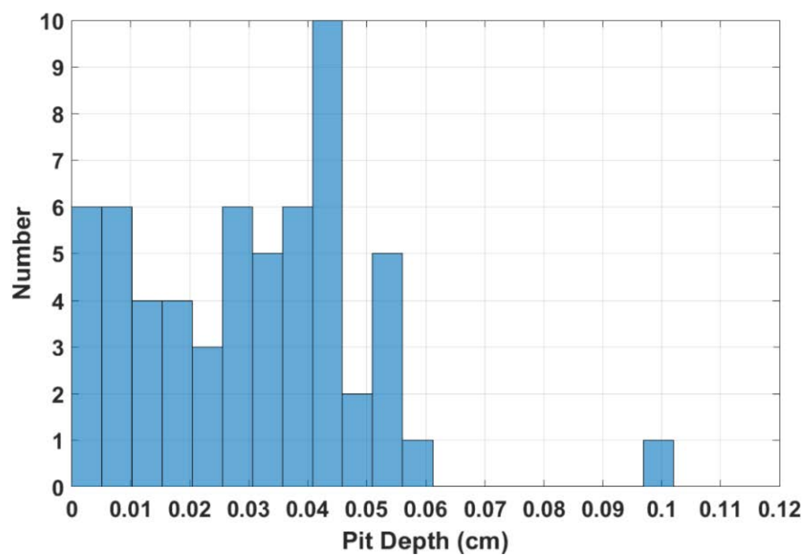

Figure 2-4
Pit depth as a function of frequency for BORAL® coupons

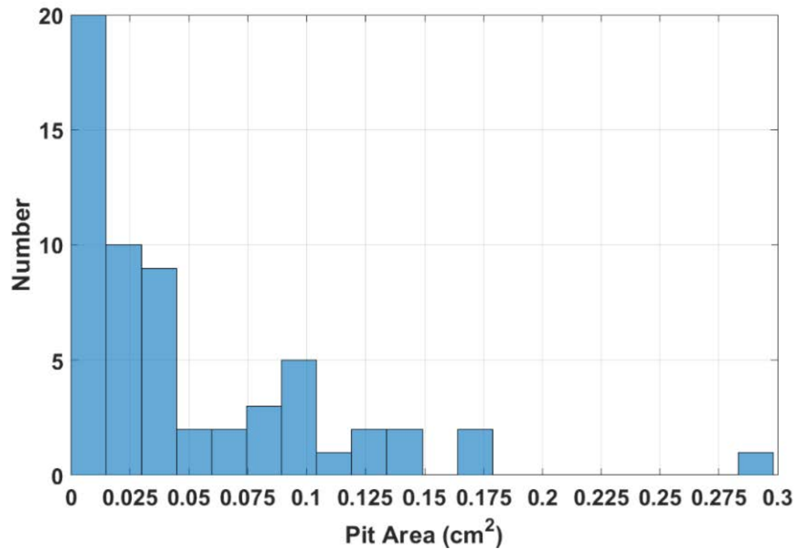

Figure 2-5
Pit area as a function of frequency for BORAL® coupons

The measured blister height and area as a function of frequency are presented in Figure 2-6 and Figure 2-7, respectively. These figures include data from over 100 coupons representing 20 SFPs with service time varying from 1 to 18 years. It should be noted that the majority of the coupons (80%) did not show any blisters. For the remaining coupons, many of them showed only a few blisters while several of the coupons showed a larger number of blisters. Based on the actual coupon data from SFPs:

- Maximum blister height is ~0.4 cm (~0.16 in.).
- Maximum blister area is ~21.4 cm^2 (~3.32 in^2).
- The blister with maximum height and the blister with the maximum area do not correspond to the same blister or even the same coupon in the same SFP.
- For the coupons with larger blister height, there was no stainless steel encapsulation, although the neutron absorber panels are typically encapsulated in stainless steel when installed on the SFP racks. The presence of encapsulation impacts the blister growth.
- The vast majority of blisters have an area less than 5 cm^2 (~0.78 in^2).

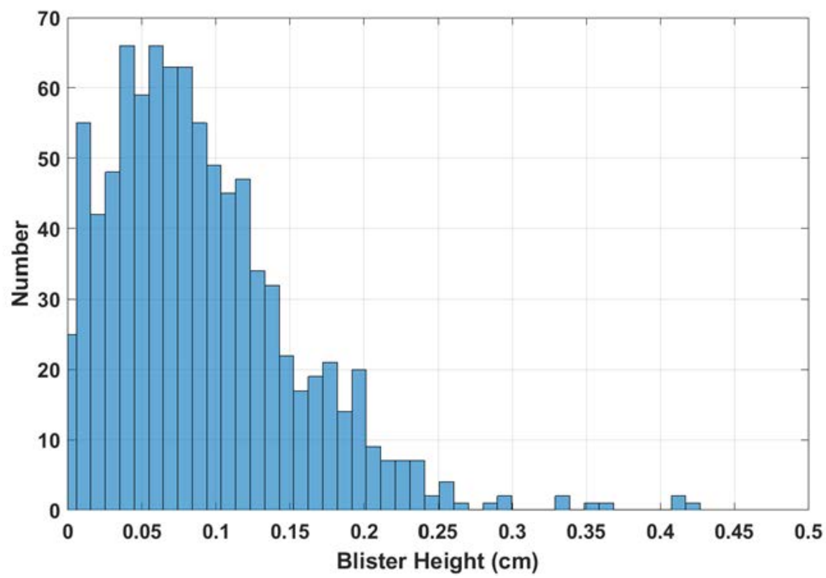

Figure 2-6
Blister height as a function of frequency for SFP coupons

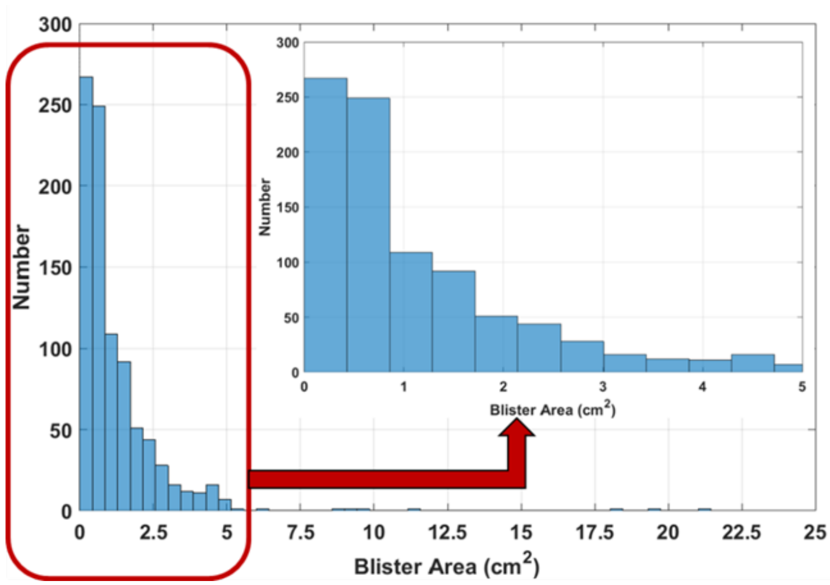

Figure 2-7
Blister area as a function of frequency for SFP coupons

It should be noted that for the coupons presented in Reference [3], despite observed blisters and pits, there was no measurable impact on neutron absorber areal density for any of the coupons.

EPRI initiated the Zion comparative analysis project to evaluate the condition of the in rack neutron absorber panels and to compare panels against neutron absorber monitoring coupons to evaluate if the coupons indeed represent the panels. The analysis showed that the Zion panels are generally in much better condition than the Zion coupons, with significantly fewer pits. Furthermore, as presented in detail in References [4-5], majority of the time, the maximum pit depth and radius do not correspond to the same pit. Consequently, the pit volume is smaller for the same pit, even when individual pit radius or depth might be relatively large. Although Zion panels were installed in 1994, there was only one small blister on one of the coupons and another one on one of the harvested panels. Neither the coupons nor the panels showed any statistically significant change in areal density [4-9].

Furthermore, the coupon analysis from EPRI's five year accelerated corrosion tests, described in References [10-12], show some blisters and pits. Accelerated corrosion tests also demonstrated the difference in blister growth for coupons with and without stainless steel encapsulation, as shown in Figure 2-8. For the coupon without encapsulation, the blister has almost a hemispherical shape and the blister height is larger, while for the coupon with stainless steel encapsulation, the height of the blister is limited to the size of the gap between the coupon and the stainless steel encapsulation. Once it reaches the stainless steel encapsulation, it flattens.

Figure 2-8
Blister growth for a coupon without stainless steel encapsulation (left) and with stainless steel encapsulation (right)

However, despite observed blisters and pits on some of the coupons, none of the coupons showed any statistically-significant change in areal density to date. This is especially important for the coupons for which the cladding was intentionally removed to evaluate the robustness of the material without a protective layer.

EPRI recently initiated the SFP coupon database project as part of its industrywide learning aging management program (i-LAMP) [13]. In Reference [13], the example of a blister growth for the same coupon in an operating SFP is also presented. After visual inspection and dimension measurements, the coupon was re-inserted to the SFP. The historic blister data from this coupon shows that after initial formation, blisters are stabilized and growth in terms of radius and height is within measurement uncertainties. As part of the i-LAMP, the data for the coupons analyzed to date for the industry are being collected and incorporated into a database that would allow expedited analysis. Subsequently, the new database will provide a larger sample size for analysis compared to the report published in 2010. The SFP coupon database is being developed with an initial focus on BORAL® but will be expanded to include other materials over time.

Section 3: Description of Rack and Fuel Assembly Geometries

The physical systems that are used in this study are described in this section. This includes descriptions of the fuel storage racks and any associated neutron absorbing panels; fuel assemblies and burnable absorbers. The fuel assembly and fuel storage rack designs considered in this report are the same as those used in Reference [14].

3.1 Fuel Assembly Descriptions

This work uses two fuel designs:

1. The Westinghouse 17x17 (W17x17) Standard fuel assembly design
2. The Combustion Engineering 16x16 (CE16x16) Standard fuel assembly design.

Both fuel designs are commonly used in pressurized water reactors (PWRs). The fuel assembly dimensions for the W17x17 and CE16x16 fuel designs are tabulated in Table 3-1. The values in parenthesis are the dimensions in inches. These two fuel assembly designs have been selected because these designs have significantly different fuel lattices based on the difference in the number and size of the water-holes. This enabled evaluation of whether the effect of blisters or pits in the neutron absorber panel is a function of fuel type.

Table 3-1
Fuel assembly dimensions

	W17x17 cm (in.)	**CE16x16 cm (in.)**
Assembly Pitch	21.5036 (8.466)	20.7772 (8.180)
Fuel Pin Pitch	1.2598 (0.496)	1.28524 (0.506)
Pellet OD	0.8192 (0.323)	0.82550 (0.325)
Cladding ID	0.8360 (0.329)	0.84328 (0.332)
Cladding OD	0.9500 (0.374)	0.97028 (0.382)
Guide Tube ID	1.1220 (0.442)	2.2860 (0.900)
Guide Tube OD	1.2240 (0.482)	2.4892 (0.980)

The isotopic inventory (and associated reactivity and neutron spectrum) of discharged fuel is impacted by the use of burnable neutron absorbers during depletion. This work includes both a fuel assembly design with significant burnable absorber loading during operation and a fuel assembly with no burnable absorbers present during operation. The W17x17 fuel design contains zirconium diboride Integral Fuel Burnable Absorbers (IFBA) and Wet Annular Burnable Absorber (WABA) during depletion while the CE16x16 contains no burnable absorbers. The burnable absorber description for the W17x17 fuel is shown in Table 3-2.

Table 3-2
Burnable absorber description

Parameter	Value cm (in.)
WABA Inner Cladding Inner Radius	0.286 (0.113)
WABA Inner Cladding Outer Radius	0.339 (0.133)
WABA Pellet Inner Radius	0.353 (0.139)
WABA Pellet Outer Radius	0.404 (0.159)
WABA Outer Cladding Inner Radius	0.418 (0.165)
WABA Outer Cladding Outer Radius	0.484 (0.191)
IFBA Coating Thickness	0.001 (0.000394)

3.2 Base Fuel Storage Rack Descriptions

The majority of the SFPs contain two types of rack designs, a flux-trap design and a high-density storage design, which will be referred to as Region 1 and Region 2 designs, respectively.

The **Region 1** design consists of stainless steel boxes which are separated from each other by a water gap (flux-trap) that provides additional reactivity hold down through neutron attenuation in the flux-trap region. The Region 1 design used for the work documented here is shown in Figure 3-1. The Region 1 design typically includes neutron absorbing panels on each storage cell wall for increased reactivity hold-down and is often used to store high reactivity assemblies.

The **Region 2** storage rack designs consist of closely-packed storage cells with shared cell walls and may contain neutron absorbing panels for reactivity hold-down. Region 2 designs allow higher density fuel storage than Region 1 designs through the use of shared cell walls, thus increasing the storage capacity of the SFP. The Region 2 design is shown in Figure 3-2. Because of the shared storage walls, Region 2 designs do not have flux-traps, and where neutron absorbing panels are used, there is only one panel between fuel assemblies.

Typically, the areal density and thickness of the neutron absorbing panels in Region 2 are lower than those typically used in Region 1. The Region 2 design typically requires fuel assemblies in this region to be less reactive (lower enrichments and/or higher fuel burnup, longer cooling time) than Region 1 designs allow.

The mechanical parameters for the Region 1 and Region 2 designs used in this study are provided in Table 3-3 and Table 3-4. In this study, four storage rack configurations that have been examined:

- Region 1 design using a neutron absorber loading of 0.015 $g^{10}B/cm^2$
- Region 2 design using a neutron absorber loading of 0.015 $g^{10}B/cm^2$
- Region 1 design using a neutron absorber loading of 0.030 $g^{10}B/cm^2$
- Region 2 design using a neutron absorber loading of 0.030 $g^{10}B/cm^2$

For comparative purposes, areal densities of 0.015 $g^{10}B/cm^2$ and 0.030 $g^{10}B/cm^2$ are used in this study for both the Region 1 and Region 2 designs.

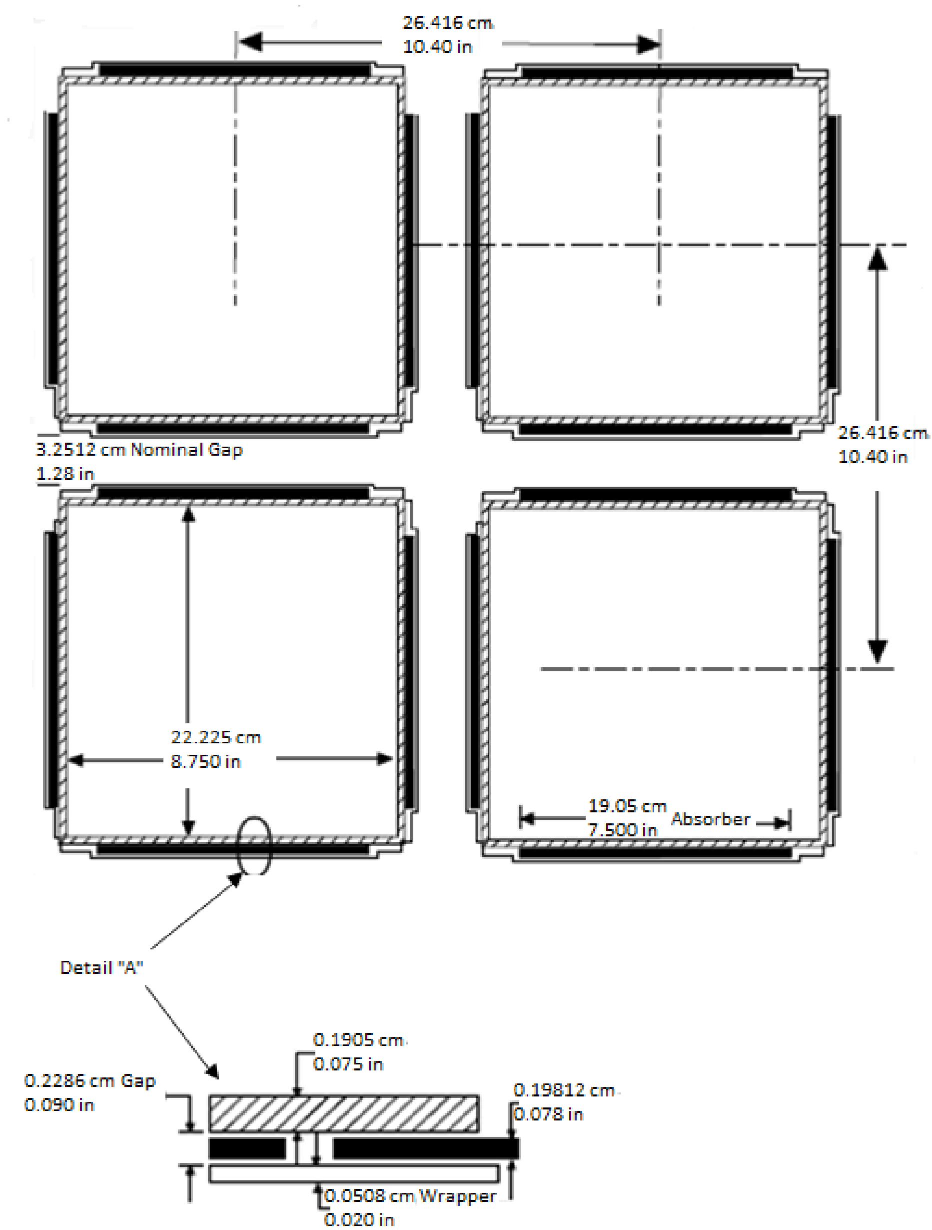

Figure 3-1
Schematic cross section of a typical PWR Region 1 rack

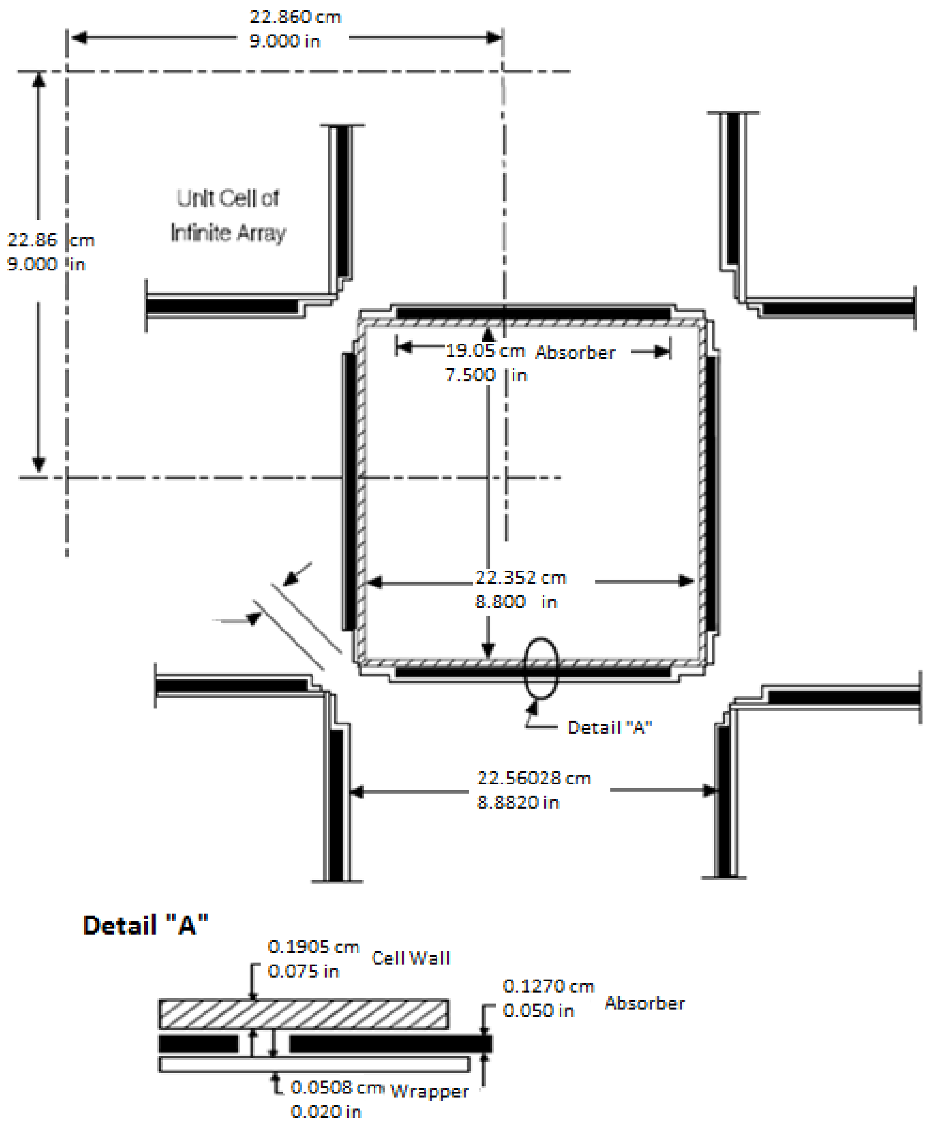

Figure 3-2
Schematic cross section of a typical PWR Region 2 rack

Table 3-3
Region 1 Fuel storage rack specifications

Parameter	Value cm (in.)
Rack Cell Pitch	26.416 (10.40)
Cell ID	22.225 (8.750)
Storage Cell Wall Thickness	0.1905 (0.075)
Flux Trap Gap	3.2512 (1.28)
Neutron Absorber Panels	
Thickness	0.19812 (0.078)
Width	19.05 (7.500)
Length	365.76 (144)
Absorber Sheath Gap	0.2286 (0.090)
Absorber Encapsulation Thickness	0.0508 (0.020)

Table 3-4
Region 2 Fuel storage rack specifications

Parameter	Value cm (in.)
Rack Cell Pitch	22.860 (9.000)
Cell ID	22.352 (8.800)
Storage Cell Wall Thickness	0.1905 (0.075)
Neutron Absorber Panels	
Thickness	0.127 (0.050)
Width	19.050 (7.500)
Length	365.76 (144)
Absorber Sheath Gap	0.16256 (0.064)
Absorber Encapsulation Thickness	0.0508 (0.020)

Section 4: Computer Codes, Nuclear Data, and Modeling Assumptions

This work requires simulation tools which evaluate the eigenvalue (k_{eff}) of spent fuel configurations in the SFP and perform fuel depletion and decay calculations. Tools performing ancillary functions such as cross section processing (for multi-group codes) and data transfer may be present to facilitate these three main functions.

4.1 Computer Codes and Nuclear Data

The analysis methodology employs the following Scale Version 6.1.2 [15] code sequences:

1. The TRITON t5-depl sequence is used to perform fuel burnup, and
2. The csas5 sequence is used to perform the reactivity calculations (rack calculations) in the SFP with the ENDF/B-VII 238-group cross section library.

The control modules, the TRITON t5-depl and general CSAS5 criticality safety analysis sequence, use following functional modules: Bondarenko AMPX Interpolator (BONAMI), Continuous Energy Transport Module (CENTRM), Produce Multigroup Cross sections (PMC), and Scale Module KENO V.a (KENO). A brief description of each module follows:

BONAMI module utilizes Dancoff approximations to perform Bondarenko unresolved resonance self-shielding calculations. BONAMI solves problems in a one-dimensional multizone slab, cylindrical, or spherical geometry. Heterogeneous effects are accounted for through the use of one dimensional (1-D) Dancoff factors evaluated for the geometry of the problem, defined as separate regions of fuel, cladding, and moderator.

CENTRM computes continuous-energy neutron spectra in zero- or one-dimensional systems, by solving the Boltzmann Transport Equation using a combination of pointwise and multigroup nuclear data. One of the major functions of CENTRM is to determine problem-specific fluxes for processing resonance-shielded multigroup data. This is done by performing a CENTRM calculation for a simplified system model (e.g., a 1-D unit cell either isolated or in a lattice by reflecting the surfaces), and then utilizing the spectrum as a problem-dependent weight function for multigroup averaging.

PMC generates problem-dependent multigroup cross-sections from an existing AMPX multigroup cross-section library, a point wise nuclear data library, and a pointwise neutron flux file produced by the CENTRM continuous-energy transport code. In the Scale sequences, PMC is used primarily to produce self-shielded multigroup cross-sections over the resolved resonance range of individual nuclides in the system of interest. The self-shielded cross-sections are obtained by integrating the point wise nuclear data using the CENTRM problem-specific, continuous-energy flux as a weight function for each spatial zone in the system.

KENO module is a multigroup Monte Carlo criticality program used to calculate the k_{eff} of 3 D models. Flexible geometry features and the availability of various boundary condition prescriptions in KENO allow for accurate and detailed modeling of fuel assemblies in storage racks, either as infinite arrays or in actual SFP models. Anisotropic scattering is treated by using discrete scattering angles through the use of Pn Legendre polynomials. KENO uses problem specific cross-section libraries, processed for resonance self-shielding and for the thermal characteristics of the problem.

4.1.1 TRITON t5-depl Sequence

The depletion model used Scale's TRITON t5-depl sequence treating the cross sections for unresolved and resolved resonances with BONAMI and CENTRM which PMC then uses to develop problem dependent multigroup cross sections. In this sequence, KENO is used for the transport (flux determination) calculation to collapse the cross sections to one energy group, using a predictor corrector time step scheme. The one-group cross sections are then used in ORIGEN-S to predict the isotopic content as a function of burnup. Despite KENO being a 3-Dimensional (3D) Monte Carlo criticality code, the model is set such that it is a 2-Dimensional (2D) analysis of an assembly in the core.

The maximum number of isotopes (388) are maintained during depletion, with an assumed cooling time of 100 hours (standalone ORIGEN-S calculation) to be representative of the peak assembly reactivity for the timeframe where an assembly would be stored in the SFP.

4.1.2 ORIGEN-S

The ORIGEN code was developed to calculate nuclide compositions and radioactivity of fission products, activation products, and products of heavy metal transmutation, and a version was implemented into the Scale code system (ORIGEN-S) to generate accurate problem-dependent cross sections for user-specified designs and conditions.

ORIGEN-S analyzes the full isotopic transition matrix through application of the matrix exponential method to solve the rate equations that describe the nuclide generation, depletion, and decay processes.

4.1.3 csas5 Sequence

The csas5 sequence uses BONAMI and CENTRM for unresolved and resolved cross section resonances and then used PMC to generate problem dependent multigroup cross sections. The KENO module is then used to perform 3-Dimensional Monte Carlo criticality calculations to determine the reactivity of the modeled system.

Of the 388 isotopes carried forth through the depletion analysis, the 185 isotopes which have a significant impact on reactivity (k_{eff}) were incorporated into the reactivity calculations performed in with the csas5 sequence. Note that any isotope containing less than $1x10^{-12}$ atoms/barn-cm was removed from the isotopic inventory carried through to the reactivity calculations.

4.1.4 Scale 6.1.2 238 Group Cross Section Library

The 238-group ENDF/B-VII library included in the Scale package is available for general purpose criticality analyses. The group structure is the same as the 238-group ENDF/B-V and ENDF/B-VI libraries in Scale, and the same weighting spectrum as for the ENDF/B-VI. As with the 238-group ENDF/B-VI library, the ENDF/B-VII library cannot be used with the NITAWL-III module for resonance self-shielding calculations in the resolved range.

The 238-group and continuous-energy ENDF/B-VII libraries have 417 nuclides that include 19 thermal scattering moderators.

4.2 Depletion Modeling and Input

Reactivity worth of blisters and pits are evaluated over a range of burnup and enrichment values. Typically, in SFP criticality analyses, analysts model fuel depletion with:

1. a uniform axial burnup profile, and
2. a limiting distributed axial burnup profile

The profile providing a higher reactivity system is used for fuel storage reactivity calculations. Results from the uniform burnup profile case typically are more limiting at low burnup, while results from the distributed burnup profile become more limiting as burnup increases.

Depletion isotopics were developed for various enrichments from 0 to 60 GWd/MTU as shown in Table 4-1 (for some enrichments, a lower maximum burnup was utilized due to the low reactivity) using both a uniform and a distributed axial burnup profile.

Table 4-1
Isotopic inventory enrichment-burnup combinations

Enrichment (wt.% ^{235}U)	Burnup (GWd/MTU)
2.0	0[1]
3.5	0[1], 10, 20, 30, 40
5.0	0[1], 20, 30, 40, 60
Notes: 1. The fuel pellets in the 0 GWd/MTU burnup step are conservatively modeled as pure UO_2 containing only the isotopes ^{235}U and ^{238}U.	

The relative axial burnup profile utilized in this work is profile 9 of Table 2 in Reference [16]. This profile is broken up into 18 equally spaces nodes and is as follows, from bottom to top as shown in Table 4-2.

Table 4-2
Axially distributed profile node-wise relative power

Node	Relative Power
1 (top)	0.284
2	0.481
3	0.614
4	0.756
5	1.022
6	1.156
7	1.190
8	1.195
9	1.192
10	1.188
11	1.189
12	1.197
13	1.208
14	1.214
15	1.215
16	1.208
17	1.044
18 (bottom)	0.649

This profile was chosen as it is the profile which has the lowest relative burnup near the fuel end, causing the largest end-effect. Additional depletion inputs are presented in Table 4-3 and Table 4-4.

Table 4-3
Depletion assumptions

Parameter	W17x17	CE16x16
Specific Power (Watts/gram of heavy metal)	38.1	38.1
Pellet Density (g/cm^3)	10.34	10.34
Fuel Temperature (K)	1050	1050
Moderator Temperature (K)	616	616
Moderator Density (g/cm^3)	0.60208	0.60208
Soluble Boron (ppm)	900	1200
Removable Burnable Absorber	20 finger WABA	None
Integral Fuel Burnable Absorber	104 IFBA rods	None

Table 4-4
Burnable absorber atom densities

WABA Pellet Atom Densities (atoms/barn-cm)	
C	0.00140923
O	0.0623784
Al	0.0415904
^{10}B	0.0029903
IFBA Coating Atom Densities (atoms/barn-cm)	
Zr	0.0322187
^{10}B	0.0215913

Using the inputs discussed in this section, the TRITON t5-depl sequence was used to develop isotopics for the W17x17 and CE16x16 fuel designs using both distributed and uniform axial burnup profiles. The isotopics inventory sets were developed at the enrichment and burnup combinations shown in Table 4-1.

4.3 Reactivity Calculation Inputs and Assumptions

To characterize the impact of potential neutron absorber panel degradation, sensitivity studies were performed comparing the reactivity of base models to the same models containing either blisters or pits. This section provides details on the modeling assumptions and simplifications used when determining the reactivity impact of blisters and pits. The modeling section is broken into discussions on the fuel assembly and fuel rack designs used in the study followed by a discussion of the modeling techniques used to represent blisters and pits.

The combinations of fuel rack and fuel assembly models without blisters or pits being incorporated are referred to as the base models. These will, unless otherwise specified, be the basis for reactivity comparisons when analyzing blisters and pits.

4.3.1 Base Model Creation

As discussed in Section 3, the study incorporates two fuel rack designs, Region 1 and Region 2, with two fuel designs: W17x17, and CE16x16. For each rack design, separate models are created with neutron absorber panels with an areal density of 0.015 $g^{10}B/cm^2$ and 0.030 $g^{10}B/cm^2$.

The following modeling approach, modeling simplifications, and modeling assumptions have been made for all of the models:

- Unborated water is used for all models unless otherwise indicated. The reason for performing the analysis for unborated water was to ensure applicability for both PWR and BWR SFPs.
- The effective multiplication factor is determined for an infinite radial array of fuel assemblies through the use of periodic boundary conditions.
- Only the active fuel length of the assembly is modeled in this analysis.
- In the active fuel length, the only assembly hardware modeled are the GTs and IT. Grids, sleeves, and top and bottom nozzles are replaced by water.
- A 50 cm water reflector is modeled above and below the storage cell (active fuel length) geometry. The SFP water is simulated to be full density (1 g/cm^3) at room temperature (20°C). The top and bottom surfaces of the water reflector have vacuum boundary conditions.
- All fuel pellets in a fuel rod are modeled as fully enriched, solid right circular cylinders, neglecting the void volume associated with pellet dishing and chamfering, and ignoring any cut-back or blanket region.
- All assembly cladding and structural material is modeled as Zircaloy-4.
- No credit is given for residual burnable absorbers; they are removed after depletion and not included in the criticality models.
- Neutron absorber panels are modeled as a material containing B_4C and Al with no Al cladding.
- Structural materials and neutron absorbers only cover the full length of the active fuel.

4.3.2 Fuel Assembly Design Modeling

The mechanical parameters for the W17x17 and CE16x16 fuel designs were presented in Table 3-1. These two fuel assembly designs have been selected because these designs are significantly different fuel lattices based on the difference in the number and size of the water-holes. However, the fuel is effectively a neutron source used to understand the sensitivity of the reactivity hold-down provided by neutron absorber panels to changes in the following:

- Neutron spectrum as shown through varying fuel enrichment, burnup, fuel assembly designs, and storage racks,
- Moderation, as shown through water displacement caused by blisters and pits, and
- Neutron absorber loss as shown by pitting of the B_4C in neutron absorber panels.

The fuel assembly designs used either represent fresh or depleted fuel. Depleted fuel contains isotopics developed with either a uniform or distributed axial burnup profile. In modeling the fuel assembly axially, the fresh fuel and uniform axial distribution models use a single axial zone while the distributed axial distribution profile uses 18 equal-length axial nodes. The isotopics for the fresh and uniform models only need a single axial zone because there is no axial variation in the isotopic inventory. These models provide a straightforward evaluation of the reactivity impact which are then supported by additional cases using models with the distributed profile. The distributed profile cases provide an understanding of the impact of the axial variability in flux and reactivity which are present in spent fuel pools.

4.3.3 Base Fuel Rack Modeling

There are two fuel rack designs used in this study, the Region 1 and Region 2 rack designs as discussed in Section 4.1 with the rack design mechanical parameters given in Table 3-3, and Table 3-4 respectively. For each rack design, two sets of models are created. One set with neutron absorber panels with an areal density of 0.015 $g^{10}B/cm^2$ and a second set with neutron absorber panels with an areal density of 0.030 $g^{10}B/cm^2$.

The Region 1 rack design detailed in Section 4.1 is radially symmetric (symmetric along the x and y axes). Therefore, the models contain a single storage cell, which is infinitely repeated using a periodic boundary conditions. A radial view of the geometry used for the Region 1 rack cases is shown in Figure 4-1.

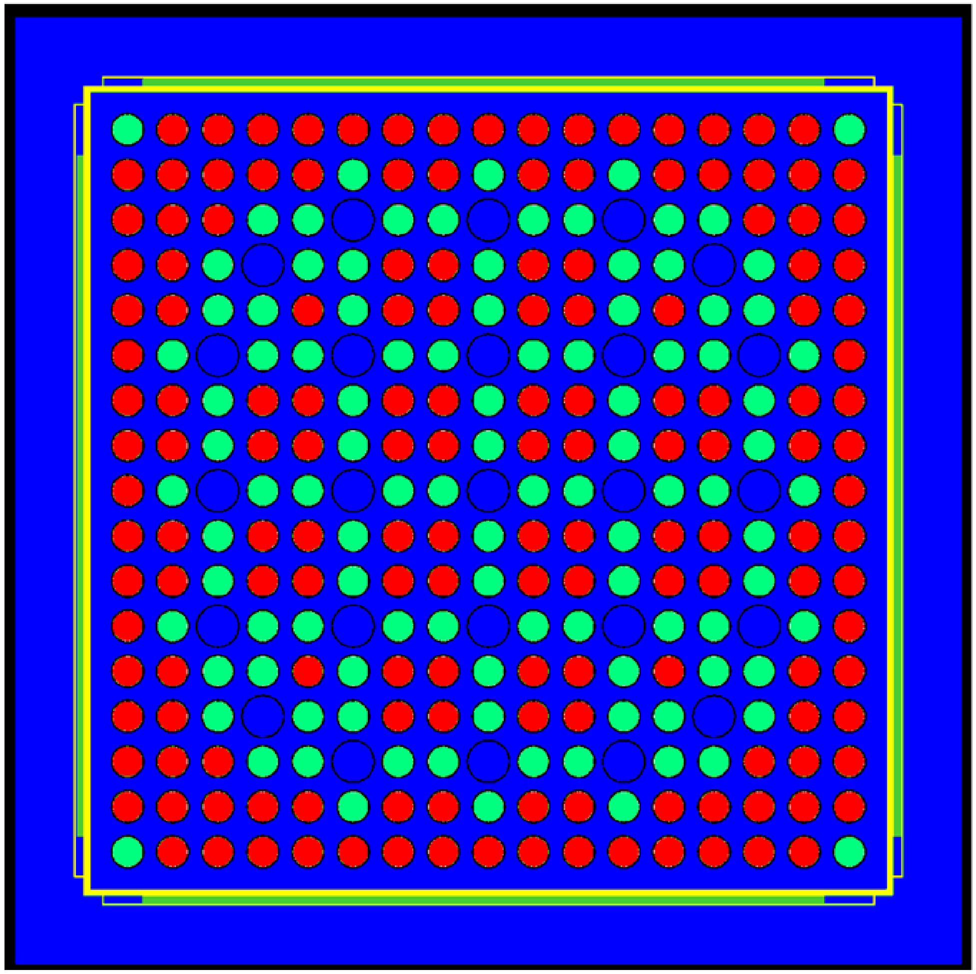

Figure 4-1
Region 1, flux trap, KENO model with W17x17 fuel

The models used to represent the Region 1 rack designs follow a standard industry assumption that only the major structures in the rack (and fuel assemblies) are included. The models include the storage cell wall, the sheathing that holds the neutron absorber panels in place, and the neutron absorber panels. The Region 1 rack component materials and absorber panel compositions are presented in Table 4-5.

The Region 2 rack design is modeled as a 2x2 array of assemblies rather than the single storage because it is not radially symmetric on a single storage cell basis. A radial view of the geometry used for the Region 2 rack cases is shown in Figure 4-2.

Table 4-5
Region 1 rack component materials

Storage Cell Wall	Stainless steel 304		Stainless steel 304	
Neutron Absorber Panel Sheath	Stainless steel 304		Stainless steel 304	
Absorber Panel Composition				
	0.015 g ^{10}B/cm^2 Areal Density		**0.030 g ^{10}B/cm^2 Areal Density**	
Isotope	$\frac{\text{Atoms}}{\text{barn}-\text{cm}}$	wt%	$\frac{\text{Atoms}}{\text{barn}-\text{cm}}$	wt%
^{10}B	0.00455268	2.85649	0.00910536	5.71297
^{11}B	0.0183251	12.6418	0.0366502	25.2836
C	0.00571945	4.30453	0.0114389	8.60906
Al	0.0474399	80.1972	0.0357212	60.3943

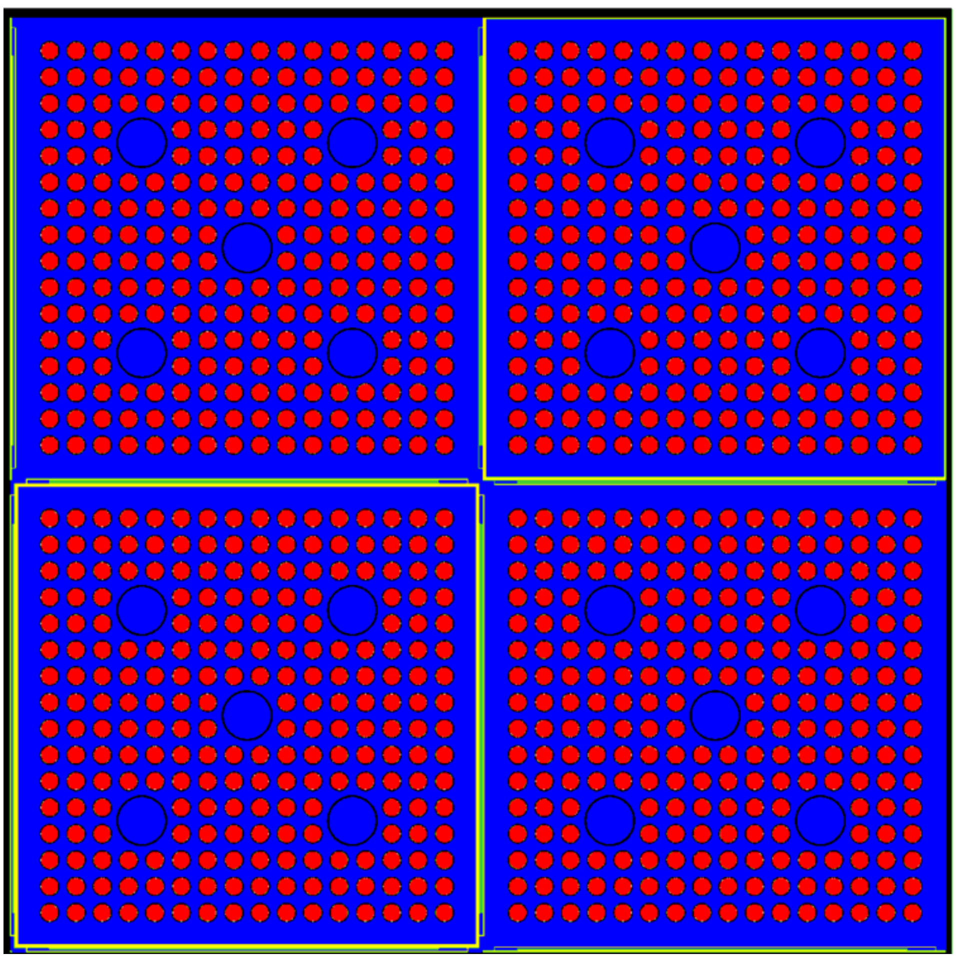

Figure 4-2
Region 2 model with CE16x16 fuel

The Region 2 rack component materials and absorber panel compositions are presented in Table 4-6.

Table 4-6
Region 2 rack component materials

Region 2 Rack Component	**Variation 1**		**Variation 2**	
Storage Cell Wall	Stainless steel 304		Stainless steel 304	
Neutron Absorber Panel Sheath	Stainless steel 304		Stainless steel 304	
Absorber Panel Composition				
	0.015 g $^{10}B/cm^2$ Areal Density		**0.030 g $^{10}B/cm^2$ Areal Density**	
Isotope	$\frac{\text{Atoms}}{\text{barn}-\text{cm}}$	wt%	$\frac{\text{Atoms}}{\text{barn}-\text{cm}}$	wt%
^{10}B	0.00710218	4.45612	0.0142044	8.91223
^{11}B	0.0285872	19.7212	0.0571743	39.4425
C	0.00892234	6.71506	0.0178447	13.4301
Al	0.0408748	69.1076	0.0226030	38.2151

4.4 Base Case Simulations

This section describes the base case simulations. Variations of these cases, called subcases contain these same base cases with differing pit and blister modeling input as well as differing isotopics for cases with burnup (uniform profile generated vs distributed profile generated isotopics). The base cases and associated parameters are given in Table 4-7 for Region 1 and Table 4-8 for Region 2.

Table 4-7
Region 1 base cases and corresponding k_{eff} values

Enrichment [wt. %]	**Burnup [GWd/MTU]**	**k_{eff}**	
		W	**CE**
Areal Density 0.015 [$g^{10}B/cm^2$]			
2.0	0	0.77871	0.75751
3.5	0	0.90216	0.87642
3.5	10	0.83780	0.80653
5.0	0	0.96795	0.93949
5.0	10	0.90183	0.87277
Areal Density 0.03 [$g^{10}B/cm^2$]			
5.0	0	0.94287	0.91754
Simulation k_{eff} Standard Deviation ≤ 12 pcm			

Table 4-8
Region 2 base cases and corresponding k_{eff} values

Enrichment [wt. %]	Burnup [GWd/MTU]	k_{eff} Areal Density 0.015 [$g^{10}B/cm^2$]		k_{eff} Areal Density 0.030 [$g^{10}B/cm^2$]	
		W	CE	W	CE
2.0	0	0.99396	0.95753	0.96363	0.93024
3.5	0	1.15240	1.10990	1.11702	1.07773
3.5	10	1.07074	1.02276	1.03796	0.99286
3.5	20	1.00549	0.95606	0.97476	0.92800
3.5	30	0.94846	0.89825	0.91964	0.87228
3.5	40	0.89982	0.84906	0.87259	0.82461
5.0	0	1.23623	1.19029	1.19846	1.15601
5.0	20	1.08948	1.04342	1.056545	1.01311
5.0	30	1.03311	0.98684	1.00201	0.95816
5.0	40	0.98160	0.93449	0.95206	0.90743
5.0	60	0.89394	0.84451	0.86696	0.82008
Simulation k_{eff} Standard Deviation ≤ 11 pcm					

4.5 Blister and Pit Modeling

A modeling strategy was developed to assess the effect of blisters and pits on the reactivity hold-down of containing B_4C and Al absorber inserts. The modeling strategy first identified the size at which either a blister or pit increases the reactivity of the modeled system by ~100 pcm. In this study pcm is defined as:

$$pcm = \frac{(k_{eff_{case}} - k_{eff_{base}})}{k_{eff_{base}}} * 10^5 \qquad \textit{Eq. 4-1}$$

where:

pcm is percent mille

$k_{eff_{base}}$ is the base case reactivity (k_{eff})

$k_{eff_{case}}$ is the perturbed case reactivity (k_{eff})

The reactivity worth of below 100 pcm is considered insignificant based on NEI 12-16, criticality guidance document [17].

The models considered increasingly extreme scenarios where blisters and pits are modeled at sizes significantly beyond current operating experience.

- For **blisters**, it is assumed that a void region is formed on the face of the neutron absorber panel, simulating the occlusion of moderator from the location containing the blister.

- For **pits**, it is assumed that the pit penetrates into the neutron absorber in the panel, replacing the absorber material with SFP water, increasing moderation while reducing the amount of absorber material.

The following nomenclature will be followed in this report when talking about blisters and pits.

- Radius will represent the size of a cylindrical blister or pit on the face of the panel.
- Width will represent the size of rectangular blisters or pits in the x or y direction (along the face of the panel).
- Length will represent the size of rectangular blisters or pits in the z-direction.
- Height will be used to represent the orthogonal distance that a blister extends from the panel face.
- Depth or thickness will be used to represent the orthogonal distance that a pit extends into the panel face.

An important aspect of both the blister and pit modeling analysis is the difference between a '***single panel***' model in Region 1 and in Region 2. The Region 1 models are a single assembly infinitely repeated where Region 2 consists of an infinitely repeated 2x2 array of assemblies. This does not impact models where all panels are being modified to include blisters or pits, however, for cases where the impact of blisters or pits is being isolated to a single panel the differences in models should be kept in mind while looking at results. For the Region 1 models, isolating the blisters or pits to a single panel causes one in four panels in the infinite array to have the defect. For Region 2, isolating blisters or pits to a single panel causes only one in twelve panels in the infinite array to have the defect. Unless otherwise stated the blisters or pits are on **all panels** surrounding the storage cell(s) in the models.

Section 5: Pitting Analysis

The modeling and analysis performed to determine the pit reactivity worth and ultimate impact on SFP criticality storage is presented in this section.

5.1 Pit Modeling

The models used to simulate the impact of pits in neutron absorber panels are the base models discussed in Section 4.3.1. The models were then modified to include a pit for single pit cases, or matrices of pits for multiple pit cases. Single pit analysis includes a pit on all panels surrounding the storage cell, unless explicitly stated otherwise.

The actual coupon data based on the operating experience from SFPs across the U.S. provided in Reference [3] indicate the maximum pit depth as 0.1016 cm (0.04 in.), as presented in Figure 2-4. Similarly, the maximum observed pit area was 0.29677 cm^2 (0.046 in^2), though not on the same pit, as illustrated in Figure 2-5. Combining the maximum depth with maximum area yields a single pit with 0.1016 cm (0.04 in.) depth and 0.307 cm (0.121 in.) radius. Since this pit is an artificial combination of the largest observed radius and depth, it bounds all neutron absorber pitting observed to date from operating experience [3].

The analysis includes both single pits and matrices of pits within the neutron absorber panels analyzed. To conservatively model the reactivity impact of pits, the following modeling assumptions have been made:

- Pits are modeled as right circular cylinders with the radius on the face of the panel, extending into the panel.
- Pits extend directly into the neutron absorber panel, replacing neutron absorber material, containing B_4C and Al, with moderator (water). Intentionally, Al cladding material is not included in the models to perform a generic study that is applicable to all metal matrix absorbers that contain a B_4C and Al mixture. By using this approach, the absorbers that contain protective cladding are penalized since pitting in the cladding is treated in these simulations as direct removal of the absorber material. As shown in Figure 2-4, in the case of BORAL®, most pits do not penetrate the Al cladding, which is approximately 0.025 cm thick [1].
- Pits are placed to be within the axial node associated with the highest source density, and determined via simulation to be at approximately the location of maximum impact. For models containing fresh and uniform profile fuel isotopics, pits are placed at the axial center of the panel. For fuel assemblies

modeled assuming a distributed profile, pits are placed near the top of the assembly as this region is identified the most reactive region for a distributed profile.

- Pits are assumed to be present in every neutron absorber panel surrounding the storage cell, unless identified as otherwise.
- Furthermore, pits are symmetrically located at the exact same axial height in each neutron absorber panel surrounding the storage cell to maximize neutron streaming.

The single pit modeling for neutron absorber panels is illustrated in Figure 5-1. In this case, **pit depth** is assumed to be **constant (0.1016 cm)**.

- For **Region 1** panels, it corresponds to removal of ~**50%** of the absorber thickness.
- **For Region 2** panels, it corresponds to removal of **~80%** of the absorber thickness.
- Pit radii varied from 0 to 9.5 cm along the panel. The panel width for both Region 1 and Region 2 is 19.05 cm. For the majority of the cases, the pit is assumed to be present on all panels surrounding the storage cell, unless otherwise stated.

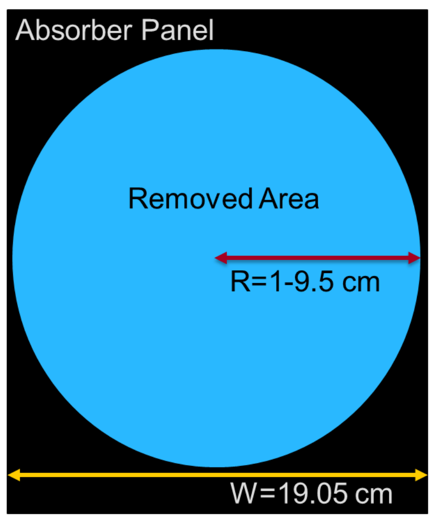

Figure 5-1
Schematic illustration of single pit modeling in neutron absorber panels

To compare the impact of a single pit versus a grid of pits, simulations were performed using distributed pitting. An example of the grid pit modeling from different perspectives is presented in Figure 5-2. In these cases, the total pit volumes were comparable to single, large radius pits. The objective of these cases was to determine if the distribution of pits has any impact because, in reality, pits are formed in clusters, with varying sizes, instead of one large pit.

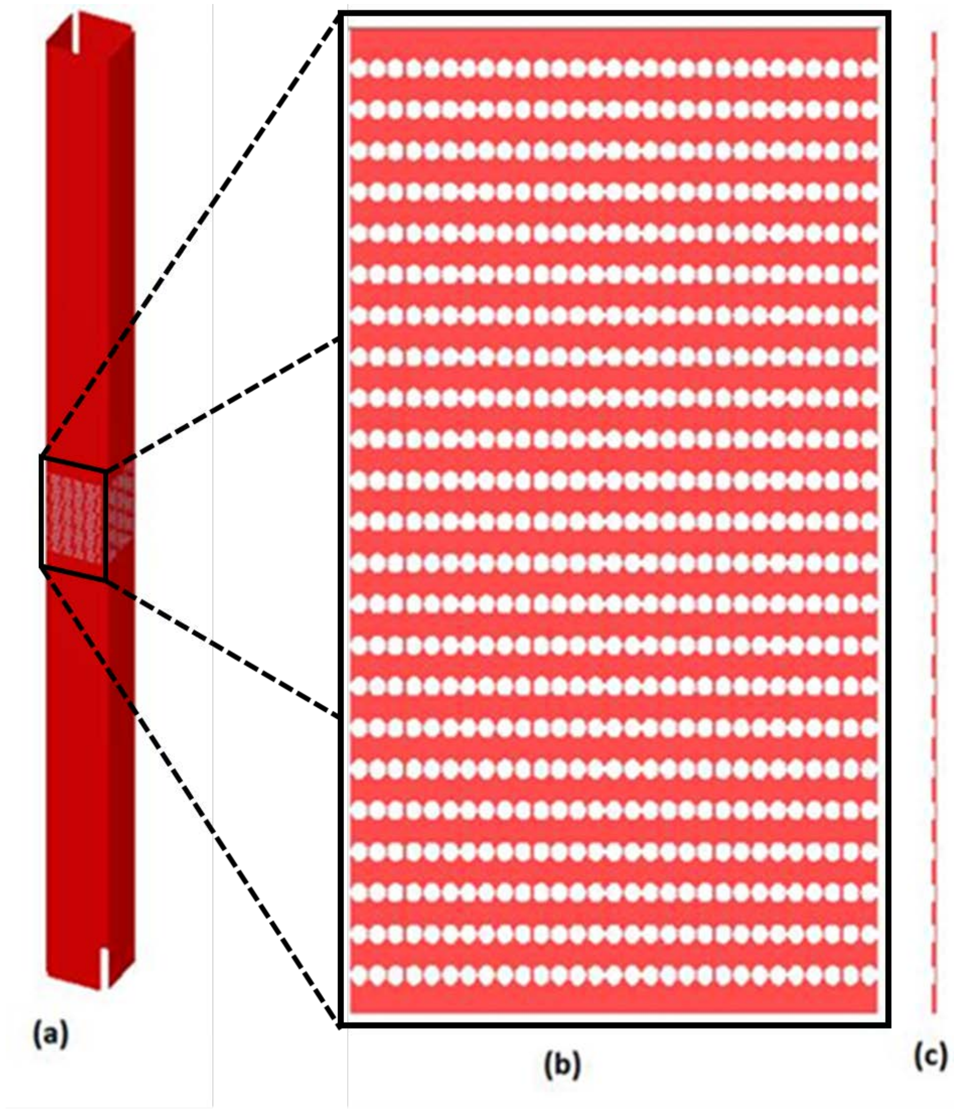

Figure 5-2
Region 1 W17x17 Keno model with a grid of pits (a) Full storage cell (b) Face view of grid pits in panel (c) profile view of the grid pit from (b)

5.2 Pit Analysis

The analysis focused on determining reactivity impact for the following cases:

- Varying pit size (radius) at the maximum observed depth that results in ~100 pcm reactivity worth.
- The number of pits of maximum observed radius with similar area to the single pit size (radius) that resulted in ~100 pcm reactivity increase.
- Impact of burnup profile on reactivity worth.

- Impact of axial location of pit formation.
- Impact of pit thickness on reactivity worth.

5.3 Single Pit Analysis

In this section, the reactivity impact of a single pit on each neutron absorber panel is analyzed. Both pit radius and depth are varied to determine the impact of pit size on the reactivity as a function of radius and depth for both W17x17 and CE16x16 fuel in Region 1 and Region 2. Fresh fuel and depleted fuel with a uniform profile are analyzed first, followed by fuel with a depleted profile.

5.3.1 Single Pit on All Panels for Fresh Fuel and Uniform Profile

A single pit was simulated for Region 1 and Region 2 configurations with various enrichment, burnup, and areal density combinations to determine the size for a single pit to yield an approximately 100 pcm reactivity increase. The pit was placed on all panels surrounding the storage cell at the same axial height, unless otherwise stated. There are 11 different burnup and enrichment combinations which have been created for the Westinghouse and CE fuel designs.

The computed k_{eff} values for the base cases for Region 1 and Region 2 racks were presented in Table 4-7 and Table 4-8, respectively. While many of the simulations are outside of the normal reactivity associated with the design bases supporting storage configurations, they still provide a good measure of reactivity worth. Further variations are not included as they would be even farther outside of the typical reactivity associated with fuel storage. For example, the eigenvalue for 2.0 wt. %, 0 GWd/MTU, 0.015 g $^{10}B/cm^2$ areal density base case is 0.77871. Clearly, for this case, even an impact of 100 pcm would not reach SFP storage criticality limits.

The reactivity impact as a function of pit radius, for a constant pit depth of 0.1026 cm (~50% of thickness for Region 1 panels), for W17x17 for varying enrichment and fixed areal density of 0.015 g $^{10}B/cm^2$ are presented in Figure 5-3. In this figure, error bars represent the 1σ uncertainty band. As described before, pits are modeled at the exact same axial height (centerline for fresh fuel) on all panels surrounding the storage cell. As shown in the figure, independent of the enrichment, the pit radius to reach ~100 pcm of pit worth, is around 6 cm for W17x17 fuel in Region 1 with an areal density of 0.015 g $^{10}B/cm^2$. As described before, the maximum observed pit radius to date from operating experience was around ~0.3 cm; therefore, the observed pits to date have no statistically significant impact on reactivity. Furthermore, the computational results also show that, compared to operating experience to date, significant margins exist until there is any measurable impact on the SFP reactivity as a pit with radius of 0.3 cm is approximately 400 times smaller than a pit with radius of 6 cm.

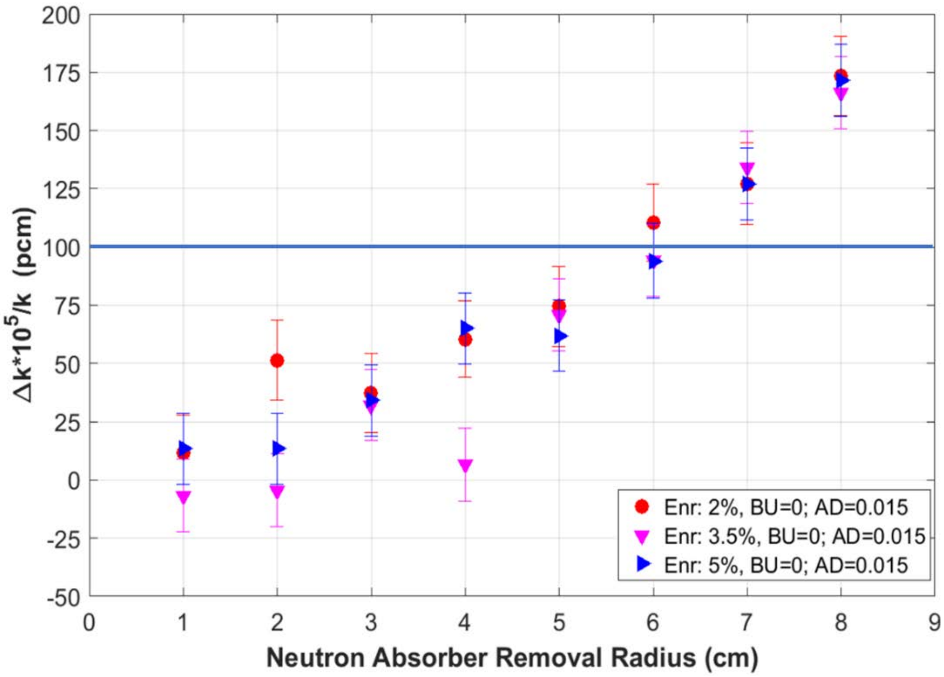

Figure 5-3
Reactivity impact of single pit, on all panels in Region 1, as a function of pit radius for a constant pit depth of ~0.1 cm, for W17x17 fuel with varying enrichment

To compare the impact of fuel type on the results, the same analysis was performed for CE16x16 fuel and the results are presented in Figure 5-4. In this figure, error bars show the 1σ uncertainty band. As shown in the figure, for CE16x16 fuel, the pit radius to reach 100 pcm reactivity worth is increased to ~7 cm. This is due to the fact that for CE16x16, the moderator to fuel ratio is higher; subsequently, there is increased moderation which impacts the change in reactivity.

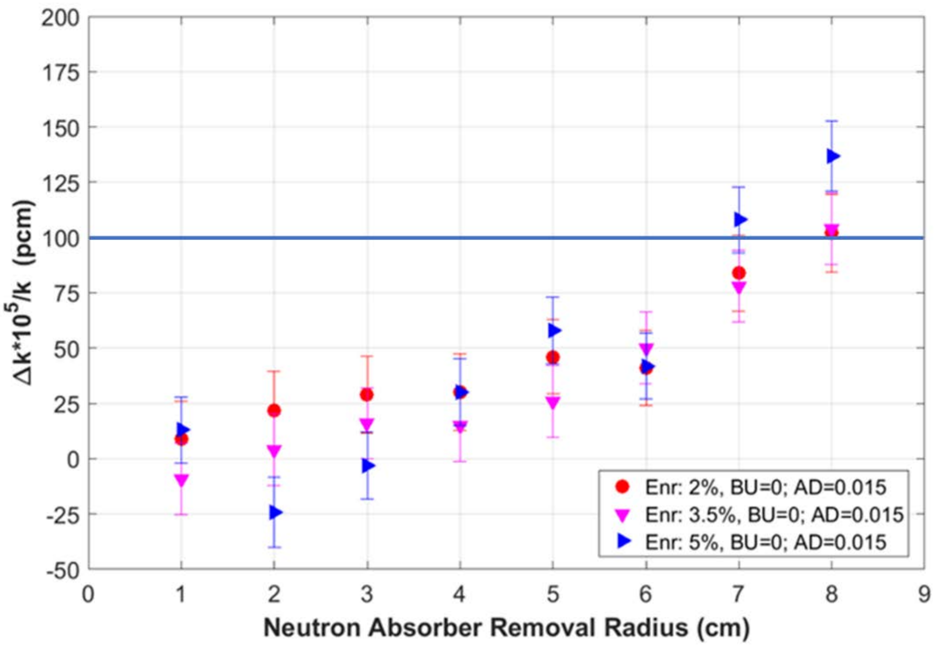

Figure 5-4
Reactivity impact of a single pit, on all panels in Region 1, as a function of pit radius, for CE16x16 fuel with varying enrichment

Figure 5-5 shows a comparison of the Westinghouse and CE fuel at areal densities of 0.015 and 0.030 $g^{10}B/cm^2$. As is evident from the figure, compared to CE16x16, the reactivity impact of pitting on neutron absorber panels is larger for W17x17 fuel. Furthermore, for the same fuel type, the impact is larger for lower absorber areal density. However, as evident from all the figures, the reactivity impact is largely a function of pit radius (and hence neutron absorber removal area) with little impact due to fuel type or panel areal density. Compared to operating experience, pits with significantly larger radius are needed to observe any measurable impact on reactivity, even for constant pit depths of 50% of absorber thickness. Error bars show the 1σ uncertainty band. In these models, pits are assumed to be present on all panels surrounding the storage cell at the exact same axial height.

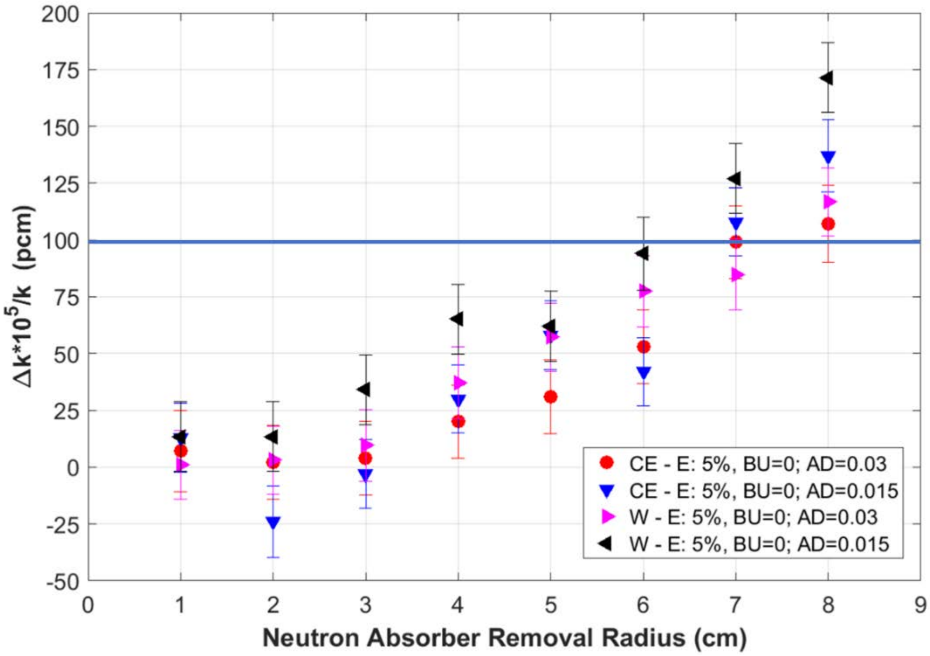

Figure 5-5
Reactivity impact of a single pit, on all panels in Region 1, as a function of pit radius, for W17x17 and CE16x16 fuels

Table 5-1 summarizes the pit radius, corresponding to approximately 100 pcm in reactivity worth for Region 1 with W17x17 fuel and CE16x16 fuel. The pit radii presented in this table correspond to a single pit that is present in all panels surrounding the storage cell at the exact same axial height, which creates a streaming path for neutrons. It should be noted that the initial analysis was performed to determine the radius that would correspond to 0.001 in Δk, after conversion to pcm, some of the values deviate from 100 pcm when divided by base k values. However, all the values are still within 2σ of 100 pcm. As is evident from the values presented in Table 5-1, to result ~100 pcm pit worth, the radius of the pit needs to be substantially larger than any observed pit to date even when:

1. Pits are present on all panels surrounding the storage cell at the exact axial height location where maximum reactivity is observed.
2. Furthermore, by assuming constant pit depth of 0.1026 cm, about 50% of the Region 1 absorber panel thickness is removed.

Table 5-1
Region 1 single pit size to reach ~100 pcm when pits are all on panels surrounding the storage cell and pit depth is 0.1026 cm (~50% of panel thickness)

Enrichment [wt. %]	Burnup [GWd/ MTU]	Areal Density [$g^{10}B/cm^2$]	W17x17		CE16x16	
			pcm	Radius (cm)	pcm	Radius (cm)
2.0	0	0.015	127.13	7.0	134.65	8.0
3.5	0	0.015	119.71	6.8	118.66	8.0
3.5	10	0.015	124.13	7.0	114.94	7.5
5.0	0	0.030	116.67	8.0	116.62	8.0
5.0	0	0.015	94.01	6.0	114.96	7.0
5.0	10	0.015	107.56	7.0	110.57	7.2
1σ ≤ 18 pcm for all cases						

The reactivity impact of the neutron absorber panel pitting, on all panels surrounding the storage cell at the same axial height, as a function of pit radius for Region 2 is presented in Figure 5-6 for 5.0 wt.% enriched W17x17 fuel. The figure shows that the reactivity impact of pits is not strongly dependent on areal density or burnup, aligning with the results provided for Region 1. In this figure, error bars represent the 1σ uncertainty band. The radius to reach ~100 pcm panel worth is around 4 cm for Region 2, as shown in Figure 5-6. The pit radius to reach reactivity worth of ~100 pcm is smaller for Region 2 (~4 cm) than for Region 1 (~6-8 cm), as shown in Figure 5-3 to Figure 5-5. However, it is important to remember that for Region 2, the assumed constant pit depth corresponds to the removal of ~80% of the neutron absorber panel thickness.

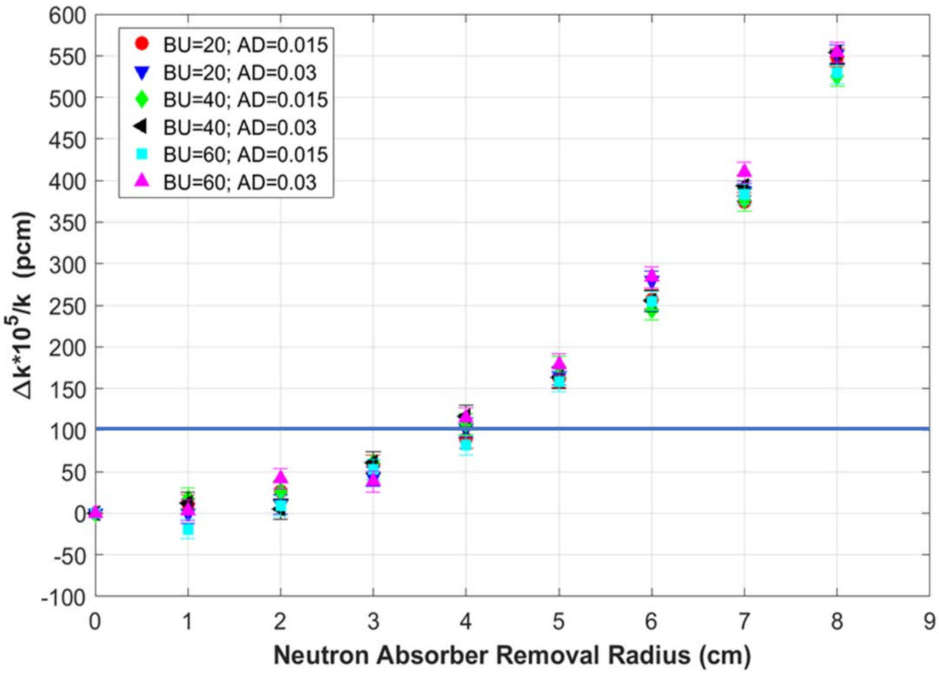

Figure 5-6
Reactivity impact of a single pit, on all panels in Region 2, as a function of pit radius, W17x17 fuel with 5% enrichment with varying burnup and areal density values

The pit radius corresponding to approximately 100 pcm in reactivity worth for Region 2 with W17x17 fuel and CE16x16 fuel are tabulated in Table 5-2. The pit radius presented in this table correspond to a single pit that is present in all panels surrounding the storage cell at the exact same axial height, which creates a large streaming path for neutrons. Data in Table 5-2 suggest that Region 2 is more sensitive to pitting than Region 1. This is to be expected for two reasons:

1. There is only a single panel with no flux-trap between assemblies in Region 2, more tightly coupling the system; and
2. The Region 2 neutron absorber panels are thinner, 0.127 cm (0.05 in.), compared to Region 1 panels with 0.19812 cm (0.078 in.) thickness. Subsequently, this difference in panel thickness cause the maximum pit depth of 0.1016 cm (0.04 in.) to be a larger percentage (~80% for Region 2 as opposed to ~50% for Region 1) of the full thickness of the panel.

As is evident from the values presented in Figure 5-6 and Table 5-2, the reactivity impact of pits is not dependent very strongly on areal density, burnup, enrichment, or fuel type. It is also important to remember that computations were performed at unborated conditions; therefore, results are not only applicable for all PWR SFPs but also for BWR SFPs.

Table 5-2
Region 2 single 100 pcm pit size determination final results (fresh or uniform profile)

Enrichment [wt. %]	Burnup [GWd/MTU]	Areal Density [g^{10}B/cm^2]	W17x17		CE16x16	
			pcm	Radius (cm)	pcm	Radius (cm)
2.0	0	0.015	102.62	4.0	114.88	4.0
2.0	0	0.030	104.81	3.6	101.05	4.0
3.5	0	0.015	85.04	3.5	81.09	3.9
3.5	0	0.030	96.69	3.8	94.65	3.75
3.5	10	0.015	96.20	4.0	94.84	4.0
3.5	10	0.030	94.42	4.0	106.76	4.0
3.5	20	0.015	102.44	4.0	108.78	4.5
3.5	20	0.030	109.77	3.7	105.60	4.0
3.5	30	0.015	101.13	4.2	106.87	4.0
3.5	30	0.030	98.05	4.0	115.79	4.0
3.5	40	0.015	111.13	4.3	116.60	4.0
3.5	40	0.030	122.62	4.1	122.48	4.0
5.0	0	0.015	80.08	3.4	116.60	4.0
5.0	0	0.030	79.27	3.5	83.04	4.0
5.0	20	0.015	89.03	4.0	87.02	3.9
5.0	20	0.030	102.69	4.0	95.74	3.6
5.0	30	0.015	105.02	3.7	97.28	4.0
5.0	30	0.030	104.79	4.0	112.72	4.0
5.0	40	0.015	116.59	4.0	96.31	4.0
5.0	40	0.030	106.97	4.0	104.58	3.95
5.0	60	0.015	114.19	4.4	121.96	4.2
5.0	60	0.030	112.98	4.0	109.75	4.0
1σ ≤ 14 pcm for all cases						

5.3.2 Single Pit Analysis for Distributed Profile

To investigate the impact of a distributed burnup profile on the pit reactivity worth, seven cases were chosen. The first case is a Region 1 simulation, with the others being Region 2 simulations. These cases include two low burnup cases and five high burnup cases. The cases used are outlined below:

- R1: W17x17 3.5 wt%,10 GWd/MTU, areal density of 0.015 g^{10}B/cm^2
- R2: W17x17 3.5 wt%, 40 GWd/MTU, areal density of 0.015 g^{10}B/cm^2
- R2: W17x17 5.0 wt%, 20 GWd/MTU, areal density of 0.030 g^{10}B/cm^2
- R2: W17x17 5.0 wt%, 60 GWd/MTU, areal density of 0.015 g^{10}B/cm^2

- R2: W17x17 5.0 wt%, 60 GWd/MTU, areal density of 0.030 $g^{10}B/cm^2$
- R2: CE16x16 5.0 wt%, 60 GWd/MTU, areal density of 0.015 $g^{10}B/cm^2$
- R2: CE16x16 5.0 wt%, 60 GWd/MTU, areal density of 0.030 $g^{10}B/cm^2$

Each fuel assembly is modeled in 18 equal length axial segments, where the source distribution is tallied. All cases with the exception of the 10 GWd/MTU case resulted in the maximum source fraction in the 2nd node from the top, with similar source fractions in the top node, and often similar source fractions in the 3rd node from the top. The maximum source in the 10 GWd/MTU case is located in the 3rd node from the top. A location sensitivity analysis was performed to determine if the selected axial location was truly the location with the maximum impact on the criticality analysis. A single pit was modeled at different axial locations in both the Region 1 and Region 2 reactivity geometries. The pit was modeled with a 5.7 cm radius for the Region 1 case and a 2.0 cm radius for Region 2 cases to determine the maximum impact location. The results of the study are presented in Table 5-3, confirming the maximum impact is within the previously modeled maximum axial source zone.

Table 5-3
Determination of the maximum axial height sensitivity

Fuel Type	Enrichment [wt. %]	Burnup [GWd/ MTU]	Areal Density [$g^{10}B/cm^2$]	Peak Impact Distance from Panel Top [cm (in.)]
Region 1				
W17x17	3.5	10	0.015	46.99 (18.5)
Region 2				
W17x17	3.5	40	0.015	27.94 (11)
W17x17	5.0	20	0.030	38.10 (15)
CE16x16	5.0	60	0.015	21.59 (8.5)
CE16x16	5.0	60	0.030	21.59 (8.5)
W17x17	5.0	60	0.015	22.86 (9)
W17x17	5.0	60	0.030	22.86 (9)

Using the results from the axial distribution study, further cases were run to identify the pit size necessary to see an approximately 100 pcm impact. The pit sizes are presented in Table 5-4. Table 5-4 also includes the impact for pits modeled in a single absorber panel in a 2x2 storage cell for comparison. Table 5-4 shows that the use of a distributed profile will increase sensitivity to the presence of pits. This is because the distributed profile used in this study is very conservative and subsequently, leads to a relatively small axial segment driving the reactivity of the assembly. Therefore, the impacts of changes within that axial region are greater than for a system with a more uniformly distributed neutronic importance to fission, and hence, reactivity.

Table 5-4
Radius for a 100 pcm impact for a single pit

Fuel Type	Enrichment [wt. %]	Burnup [GWd/MTU]	Areal Density [$g^{10}B/cm^2$]	Pit Radius (cm) for Pit Worth of ~100 pcm		
				All Panels Uniform	All Panels Dist.	1 Panel Dist.
Region 1						
W17x17	3.5	10	0.015	7.0	3.8	> 9.5
Region 2						
W17x17	3.5	40	0.015	4.3	1.9	5.7
W17x17	5.0	20	0.030	3.6	2.3	6.0
CE16x16	5.0	60	0.015	4.2	1.8	5.4
CE16x16	5.0	60	0.030	4.0	1.9	5.5
W17x17	5.0	60	0.015	4.4	2.0	5.5
W17x17	5.0	60	0.030	4.0	1.8	5.3
$1\sigma \leq 11$ pcm for all cases						

The single panel case represents the reactivity impact of a single pit at the height of maximum neutronic importance. In reality, it would not be likely to have pits that are symmetrically aligned on every panel at the height of maximum neutronic importance to create streaming windows. As is evident from the values provided in Table 5-4, the single panel case further demonstrates that the reactivity impact of a single pit is much lower than multiple symmetrically aligned pits. The reduction in reactivity worth is not linear. Therefore, the '**all panels**' cases result in a significant penalty that is far beyond operational experience or expected pitting mechanisms.

5.4 Multiple Pits Analysis

The initial pitting analysis assumes large radius pits, either on all panels or only one panel surrounding the storage cell. This provides a relationship between pit area and reactivity change at a constant pit depth. To determine whether it is more penalizing to model a single large pit or multiple small pits, simulations were performed using multiple pits in a grid structure to compare against the single pit results.

The maximum in-service pit area observed corresponds to a pit radius (assuming cylindrical pits) of 0.3074 cm as determined in Reference [3]. Three models are simulated. Each of these models contains a grid of pits with the maximum observed in-service pit radius and thickness based on the operating experience to date [3]. It should be noted that the maximum pit depth and pit radius do not correspond to the same pit in this case. Therefore, the analysis performed by combining two worst case observations. The total number of pits is set to yield a similar total area to the single pit areas presented in Table 5-1 and Table 5-2. The three pit grid structures chosen for each case correspond with:

1. Closely packing pits in each row of pits to create alternating horizontal strips of pits and panel sections;

2. Closely packing pits in each column to create alternating vertical strips of pits and panel sections;

3. A grid structure approximately evenly spaced in the radial and axial directions.

These models will provide variability to assess worth with different pit locations with approximately the same number of pits. To illustrate, a wireframe model of a single absorber panel is shown for grid structures of 29x13 (377 pits, left), 49x8 (392 pits, middle) and 15x25 (375 pits, right) as shown in Figure 5-7. The positioning of the pit rows and columns were calculated to fit within approximately 30 cm (12 in.) in axial height and 19 cm (7.5 in.) in length.

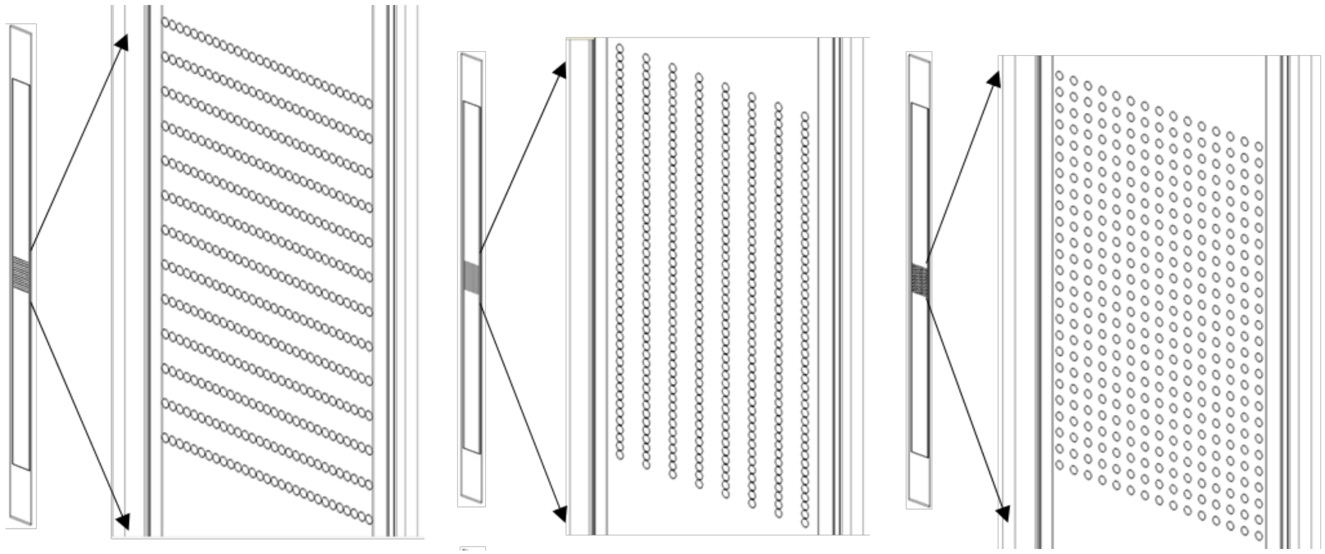

Figure 5-7
Neutron absorber panel with 29x13 rectangular grid pits (left) and 49x8 (middle), 15x25 (right)

5.4.1 Fresh Fuel and Uniform Profile

For the fresh fuel and uniform burnup profile cases evaluated here, reactivity is driven by the center of the fuel assembly, and as such, the multiple pits modeled are initially limited to the middle 30 cm of the fuel assembly. For Region 1, four total cases from Table 5-1 were selected corresponding with the smallest pit sizes shown to approximately equal 100 pcm. Results are presented in Table 5-5.

Table 5-5
Region 1 multiple pit sensitivity analysis

Fuel Type	Enrichment [wt. %]	Burnup [GWd/MTU]	Areal Density [g^{10}B/cm^2]	Rows	Columns	pcm
W17x17	3.5	10	0.015	18	29	97.88
				49	11	107.42
				29	18	95.49
W17x17	5.0	0	0.030	23	29	119.85
				49	14	83.79
				33	21	99.70
W17x17	5.0	0	0.015	13	29	63.02
				49	8	73.35
				25	15	80.58
CE16x16	5.0	0	0.015	18	29	61.74
				49	11	69.19
				29	18	61.74
1σ ≤ 17 pcm for all cases						

The same procedure was used for Region 2 based on results given in Table 5-2. For Region 2, six total cases from Table 5-2 were selected for further sensitivity analysis. The four W17x17 and two CE16x16 cases which required the smallest pit sizes to cause an approximately 100 pcm reactivity impact from Table 5-2 were selected. Results are presented in Table 5-6.

Table 5-6
Region 2 multiple pit sensitivity analysis

Fuel Type	Enrichment [wt. %]	Burnup [GWd/MTU]	Areal Density [g^{10}B/cm^2]	Rows	Columns	pcm
W17x17	2.0	0	0.030	5	27	57.35
				49	3	64.39
				15	9	78.47
W17x17	3.5	0	0.015	5	26	51.20
				49	3	64.21
				14	9	44.26
W17x17	5.0	0	0.015	5	30	60.67
				49	3	80.89
				15	10	54.20
W17x17	5.0	0	0.030	5	26	69.26
				49	3	60.08
				14	9	65.08
CE16x16	3.5	0	0.030	5	26	49.18
				49	3	62.17
				14	9	59.38
CE16x16	5.0	20	0.030	5	27	55.28
				49	3	76.99
				15	9	76.00
1σ ≤ 13 pcm for all cases						

As is evident from the values presented in Table 5-5 and Table 5-6, the single pit model tends to overpredict the overall pit reactivity worth for the total pit area (at 0.1016 cm depth). The single pit model provides a larger penalty for overall representation of the reactivity impact for fresh fuel and uniform burnup profile models. When a single large radius pit is compared against a grid of pits with smaller radii, there is still intermittent neutron absorber material present for the grid pit case, as shown in Figure 5-7 compared to Figure 5-1, even for equivalent pitting areas. For the grid pit case, some of the neutron absorber material is still present within the grid structure; subsequently, neutrons avoid some of the streaming path. Consequently, the probability of absorption in the panel for the grid pitting scenario is higher compared to the large single pit case.

5.4.2 Distributed Profile Cases

With the refinement of the axial location of maximum impact for the single pit radius determination, cases were run with multiple pits at this axial location, updating the multiple pit data to be associated with the maximum pit impact location. Calculations are performed to assess the reactivity impact for pits of the maximum observed radius and depth. Results are presented in Table 5-7. The data in Table 5-7 suggest, similar to the fresh fuel and uniform burnup profile associated simulations, that the pit worth is reduced when using multiple smaller pits compared to a single pit of equivalent area for pits of the maximum observed depth (volume). As a result, the single pit case at the maximum impact location bounds the multiple pit case. Based on the coupons from operational experience to date [3] and Zion coupon and panel data [4-9], pits are usually distributed and are not formed as one large pit covering the entire region.

Table 5-7
Multiple pit sensitivity analysis – distributed profile

Fuel Type	Enrichment [wt. %]	Burnup [GWd/MTU]	Areal Density [$g^{10}B/cm^2$]	Rows	Columns	pcm
W17x17	3.5	10	0.015	16	10	78
W17x17	3.5	40	0.015	8	5	30
W17x17	5.0	60	0.015	8	5	7
W17x17	5.0	60	0.030	7	5	30
CE16x16	5.0	20	0.030	10	6	10
CE16x16	5.0	60	0.015	7	5	53
CE16x16	5.0	60	0.030	8	5	44
$1\sigma \leq 17$ pcm for all cases						

In Sections 5.1 and 5.2 it has been assumed that the maximum reactivity impact will be seen at the maximum source location. The maximum reactivity location corresponds to the fuel mid-plane for fresh fuel and fuel with a uniform axial profile and towards the top of the fuel assembly for fuel with a distributed axial profile. This section alternatively validates this assumption and assesses the reactivity impact of the axial locations of pits. To accomplish this, pit models for the distributed profile are expanded from being 30.48 cm (12 in.) to one third, two thirds, and full panel length, changing the spacing between individual pits in the grid. As an illustrative example, a 33x21 grid of pits will be modeled covering the middle 30.48 cm (12 in.), center one third, center two thirds, full panel, top 30.48 cm (12 in.) and top one third). Models chosen for expansion are identified in Table 5-8 including the grid pit structure (R=Rows, C=Columns) assumed.

Table 5-8
Distributed profile expanded pit analysis subcase descriptions

Case ID	Fuel Type	Enrichment [wt. %]	Burnup [GWd/MTU]	Areal Density [$g^{10}B/cm^2$]	Grid Pit (R x C)
A	W17x17	3.5	10	0.015	29x18
B	W17x17	3.5	40	0.015	18x11
C	W17x17	5.0	60	0.015	18x11
D	W17x17	5.0	60	0.030	17x10
E	CE16x16	5.0	20	0.030	15x9
F	CE16x16	5.0	60	0.015	17x11
G	CE16x16	5.0	60	0.030	17x10

Pit size for this analysis was associated with the radii from the fresh fuel and uniform profile analysis and is only meant to show the overall change in reactivity worth for pits at different panel locations. Results for these cases/subcases are presented in Table 5-9.

The data in Table 5-9 suggest that the worth of pits is heavily dependent on the neutronic importance of the axial fuel region. Compared to fresh fuel cases, where the center of the fuel is important; for the distributed profile cases, the center of the panel is negligible. However, as pit sizes are expanded to the panel end, worth starts to increase. Additionally, the spacing between pits is shown to be important as can be seen from the significant reactivity differences between the top 30 cm and top 1/3 panel cases for high burnup fuel compared to the other cases. In general, cases using a distributed burnup profile yield a higher pit impact than the similar fresh fuel and uniform burnup profile cases (at the maximum pit depth observed in service). This also should be dependent on the distributed profile used in the analysis. For this study, a very conservative profile from Reference [16] is chosen.

Table 5-9
Pit axial expansion sensitivity analysis (distributed burnup profile isotopics)

Case	Middle 30 cm [pcm]	Middle 1/3 Panel [pcm]	Middle 2/3 Panel [pcm]	Full Panel [pcm]	Top 1/3 Panel [pcm]	Top 30 cm [pcm]
A	-24	17	28	43	142	133
B	2	-14	17	49	131	248
C	-7	19	-26	41	105	300
D	3	14	7	44	111	282
E	-31	-15	-17	22	98	124
F	1	-22	0	25	114	280
G	10	17	5	37	103	279
1σ ≤ 17 pcm for all cases						

5.5 Worth of Pitting in One Panel

The analyses performed to this point used models in which the pits are repeated symmetrically in every absorber panel in the model. This assumption bounds the reactivity impact of pits. In this section the highest reactivity worth cases will be modified to model pits only in a single panel in each model. The difference between the Region 1 and Region 2 model sizes means that for Region 1, one in four panels will have a pit, where Region 2 will have pits in one of every twelve panels.

In general, cases using a distributed burnup profile yield a higher pit impact than the similar fresh fuel and uniform burnup profile cases (at the maximum pit depth observed in service). The first case (3.5 wt. % 10 GWd/MTU) in Table 5-5 is evaluated for both the uniform and distributed profile subcases. The results of the fresh fuel and uniform burnup profile cases when pits are modeled in a single absorber panel are presented in Table 5-10 and Table 5-11 for Region 1 and Region 2, respectively. The pit size was expanded until a reactivity impact was ~100 pcm (including the calculational uncertainty) or a pit radius of 9.5 cm was reached. Pit radii larger than 9.5 were not used since the width of the neutron absorber panels used in this study limits the maximum achievable pit radius to 9.525 cm.

Table 5-10
Single panel, single pit reactivity worth analysis for Region 1 panels with fresh fuel / uniform burnup profile subcases

Fuel Type	**En. [wt. %]**	**Burnup [GWd/MTU]**	**Areal Density [$g^{10}B/cm^2$]**	**Pit Radius [cm]**		**Panel Worth [pcm]**	
				All Panels	**Single Panel**	**All Panels**	**Single Panel**
W17x17	3.5	10	0.015	7.0	>9.5	124	11
W17x17	5.0	0	0.030	8.0	>9.5	117	11
W17x17	5.0	0	0.015	6.0	>9.5	94	19
CE16x16	5.0	0	0.015	7.0	>9.5	115	0
1σ ≤ 17 pcm for all cases							

Table 5-11
Single panel, single pit reactivity worth analysis for Region 2 panels with fresh fuel / uniform burnup profile subcases

Fuel Type	**En. [wt. %]**	**Burnup [GWd/MTU]**	**Areal Density [$g^{10}B/cm^2$]**	**Pit Radius [cm]**		**Panel Worth [pcm]**	
				All Panels	**Single Panel**	**All Panels**	**Single Panel**
W17x17	2.0	0	0.015	3.6	>9.5	105	97
W17x17	3.5	0	0.015	3.5	>9.5	85	90
W17x17	5.0	0	0.015	3.4	>9.5	80	84
W17x17	5.0	0	0.030	3.5	>9.5	79	91
CE16x16	3.5	0	0.030	3.75	>9.5	95	63
1σ ≤ 13 pcm for all cases							

Results for pits in a single panel show that the reactivity impact is lower than the quantified maximum impact values in Section 5.2 for pits in all panels placed symmetrically. This study was extended to multiple pits (radius 0.3074 cm, depth 0.1016 cm) in a single panel to confirm whether the same conclusions held when a panel contained multiple pits.

Table 5-12 contains the results of this study which show that multiple pits in a single panel yield similar worth for the Region 1 fresh fuel and uniform burnup profile subcases.

Table 5-12
Region 1, single panel, single and multiple pit (39x24 grid) reactivity worth comparison, fresh fuel / uniform burnup profile subcases

Fuel Type	Enrichment [wt. %]	Burnup [GWd/MTU]	Areal Density [g^{10}B/cm^2]	Single Pit [pcm]	Multiple Pits [pcm]
W17x17	3.5	10	0.015	10.9	-4.1
W17x17	5.0	0	0.030	10.6	-2.1
W17x17	5.0	0	0.015	18.6	19.6
CE16x16	5.0	0	0.015	0.0	-2.1
1σ ≤ 17 pcm for all cases					

Table 5-13 shows a comparison of the single and multiple pit reactivity impacts for distributed profile cases in Region 1 and Region 2 (Single pit radius from Table 5-4). These results show that there is a reduction in reactivity impact between 33 and 90 percent when transitioning from models assuming a single pit to a grid of pits of the maximum observed size.

Table 5-13
Select maximum impact single panel, single and multiple pit reactivity worth comparison, distributed profile (Region 1 and 2)

Fuel Type	Enrichment [wt. %]	Burnup [GWd/MTU]	Areal Density [g^{10}B/cm^2]	Single Pit [pcm]	Multiple Pits [pcm]
Region 1					
W17x17	3.5	10	0.015	37.6	28.4
Region 2					
W17x17	3.5	40	0.015	94.1	38.8
W17x17	5.0	60	0.015	107.4	42.4
W17x17	5.0	60	0.030	114.5	49.5
CE16x16	5.0	20	0.030	86.3	8.9
CE16x16	5.0	60	0.015	113.1	35.8
CE16x16	5.0	60	0.030	110.0	47.2
1σ ≤ 17 pcm for all cases					

5.6 Impact of Pit Depth on Reactivity Worth

Evaluation of the impact of pitting on reactivity thus far focused on pits of the maximum depth observed to date based on the recorded operating experience [3]. Furthermore, it is assumed that the neutron absorber material does not have any protective cladding material; therefore, the maximum depth corresponds only to removal of the absorber material, ignoring the protection afforded neutron absorbers with cladding. The observed maximum depth to date corresponds to ~50% of the panel thickness for the neutron absorber material used in Region 1 and ~80% through the Region 2 panels used in this study. This section focuses on reactivity impact of pitting as a function of pit depth.

To evaluate the impact of pitting as a function of pit depth, the pit depth was varied from zero to one hundred percent of the panel thickness. The reactivity worth as a function of depth was investigated for:

- Single pit on all neutron absorber panels surrounding the storage cell
- Grid pits on all panels surrounding the storage cell with pitting area approximately equal to single pit cases
- For a single pit in a single panel with radius of up to a maximum of 9.5 cm.

The reactivity worth as a function of absorber thickness removal, in percentage, for the limiting Region 1 case, W17x17, 5.0 wt. %, 0 GWd/MTU, and 0.030 $g^{10}B/cm^2$ for these three pit configurations is presented in Figure 5-8. This is the limiting case as it contains the highest weight percent fuel with the highest areal density panel, and the single pit model actually contains a pit in every panel, all aligned at the exact axial height for streaming. The full thickness worth for the single pit fresh fuel model for this case is approximately double of any other case evaluated.

In this configuration, a single pit on all panels corresponds to a pit with an 8 cm radius placed on all panels surrounding the storage cell at the exact same axial location. Grid pitting corresponds to modeling pits on all panels at the same height assuming a distribution of 21x33. Finally, a single pit on a single panel corresponds to a pit with a radius of 9.5 cm. As is evident from Figure 5-8, when a pit with radius of 8 cm is placed at the same exact axial height on all absorber panels surrounding the storage cell, the reactivity worth is significant when 100% of the absorber is removed. However, this case not only assumes pit size is very large (~30 times higher than maximum pit radius observed to date) but also assumes pits are aligned, creating a perfect streaming path and 100% of the absorber is lost. Even when a large pit is considered as a single pit on a single panel, the impact is substantially reduced, as shown in the figure. For grid pit modeling, even though it is assumed that pits are symmetric on all panels, it still shows that the impact is significantly lowered compared to large pits on all panels. The pit worth as a function of absorber thickness removal for absorber thickness removal of up to 60% is shown in the inset of Figure 5-8. In this figure, 100 pcm is marked with a dark blue line. As is evident from the figure, when pits are placed on all panels, ~45% of removal corresponds to 100 pcm. However, for a single pit on single panel, even with radius of 9.5 cm, the impact is within the statistical fluctuations; hence, negligible.

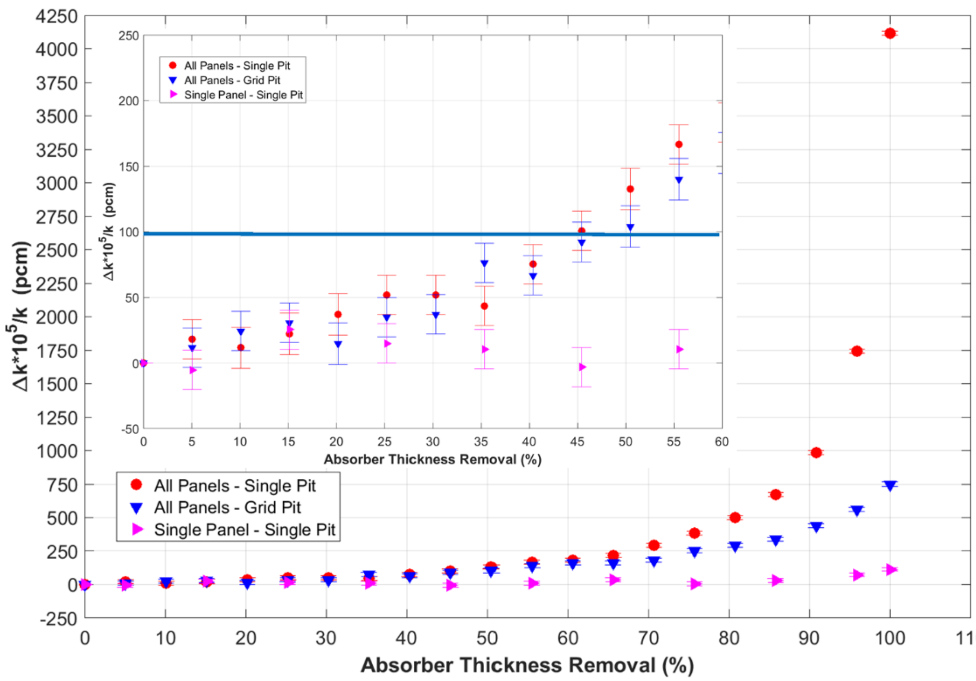

Figure 5-8
Impact of pit depth for Region 1 panels with a pit radius of 8 cm for pits on all panels and 9.5 cm for a single panel, grid pit modeling assumes 21x33 pitting structure; all three cases assume limiting fresh fuel/uniform profile case (W17X17, 5.0 wt. %, 0 GWd/MTU, 0.030 g^{10}B/cm^2)

To further analyze the impact of the geometric distribution of pits on the reactivity, an additional case was modeled. In this case, pits are distributed across the entire panel more coarsely while for each pit 100% of the absorber was removed. The geometry for an absorber panel with the 21x33 grid pit, distributed around the center versus 6x115 grid pit model, pits distributed across the entire panel, is presented in Figure 5-9. The comparative results are presented in Table 5-14. As is evident from the values presented in the table, the geometric distribution of the pits has a significant impact on the reactivity worth. Even for the largest radius, if the pits are not perfectly aligned, the impact is substantially lower.

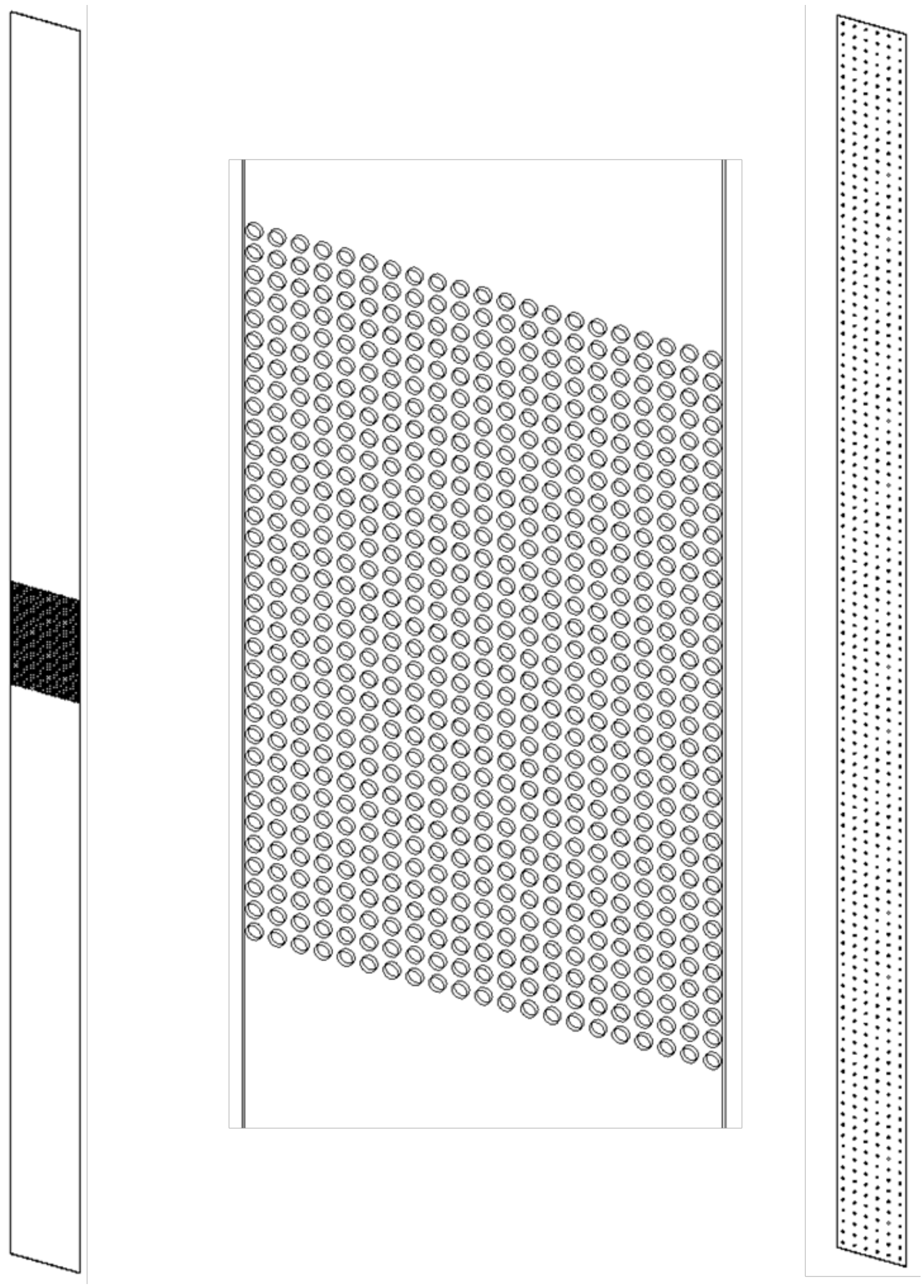

Figure 5-9
Neutron absorber panel grid pit model, 21x33 pits axially centered within 15.24 cm of the fuel midplane (left), zoomed portion of the center 30.48 cm of the 21x33 grid pit model (middle), and 6x115 absorber panel grid pit model evenly distributed throughout the absorber panel (right)

Table 5-14
Comparison of the impact of pitting geometry on reactivity worth for 100% neutron absorber thickness removal for Region 1 neutron absorber panels

Case	Pit Worth ± 1σ [pcm]
Single pit on all panels at the same axial height, pit radius=8 cm	4116 ±16
Grid pit (21x33) on all panels, distributed around center (Figure 5-9-b)	749 ±15
Grid pit (6x115) on all panels, distributed across entire panel (Figure 5-9-c)	229 ±15
Single pit on single panel, pit radius=9.5 cm	113 ±15

The pit worth as a function of pit depth for fresh fuel/uniform profile case for W17x17 fuel with 5.0 wt. % enrichment, 0 GWd/MTU burnup, and 0.030 $g^{10}B/cm^2$ areal density for Region 2 is presented in Figure 5-10. In this figure, a single pit with radius of 3.5 cm in all absorber panels, at the exact same axial height, is compared against a single pit in one absorber panel for radius of 3.5 cm and 9.5 cm. The error bars represent the 1σ uncertainty band and the line in dark blue shows the 100 pcm pit worth. As is evident from the figure, for a single pit with radius of 3.5 cm on one panel, the impact on reactivity is insignificant, within statistical fluctuations, even for 100% thickness removal. For the same radius, 3.5 cm pit size, the reactivity worth is substantially lower compared to pits on all panels.

The comparative analysis of a single pit on all panels against a grid of pits (9x14) on all panels for similar area at the exact same axial height is presented in Figure 5-11. As is evident from the figure, the pit impact is reduced with the grid pit structure. The reduction is not as substantial as the previous case since in this grid distribution, pits are still clustered heavily around the center and not very coarsely distributed.

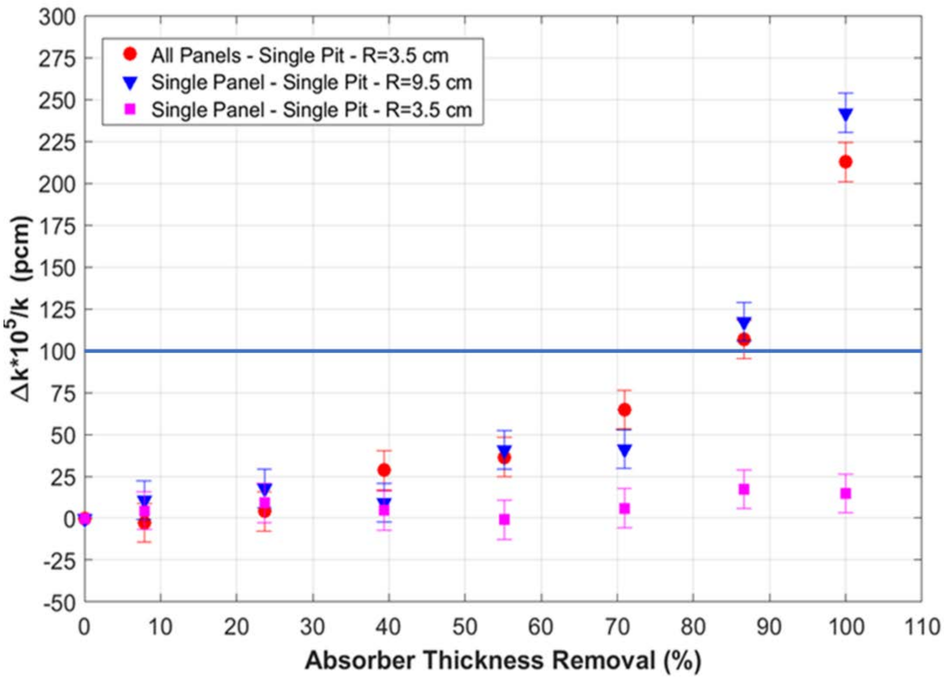

Figure 5-10
Region 2 pit depth comparison for fresh fuel/uniform profile case for W17x17 fuel 5.0 wt. % enrichment, 0 GWd/MTU, 0.030 g^{10}B/cm^2 for a single pit in all absorber panels with radius 3.5 cm, and for a single pit in one absorber panel for radius of 3.5 cm and 9.5 cm

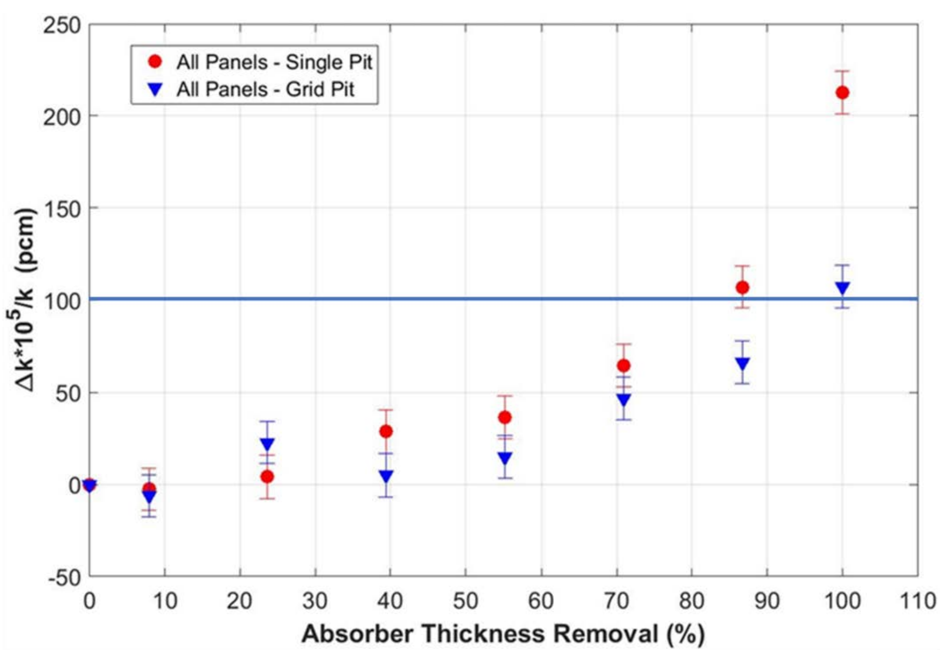

Figure 5-11
Region 2 pit depth comparison for a single pit in all absorber panels versus grid pit (9x14) in all absorber panels surrounding the storage cell

The impact of absorber thickness removal for Region 1 using a distributed profile for W17x17 fuel with 3.5 wt. % enrichment, 10 GWd/MTU burnup, and 0.015 $g^{10}B/cm^2$ areal density is presented in Figure 5-12. In this case, the pit radius for a single pit, assumed on all panels surrounding the storage cell at the same axial height, is 3.8 cm. The single pit on all panels compared against 10x16 grid pitting on all panels, at the same axial location, yields a similar area. In the distributed case, the pits are placed at the maximum impact location, instead of at the center. 100 pcm impact is reached when about 45% of the thickness is removed. Especially beyond 75% of thickness removal, the reactivity impact for grid pit is lower, compared to single pit. As is evident from the figure, the impact for the grid pitting is approximately three times lower at 100% absorber thickness removal.

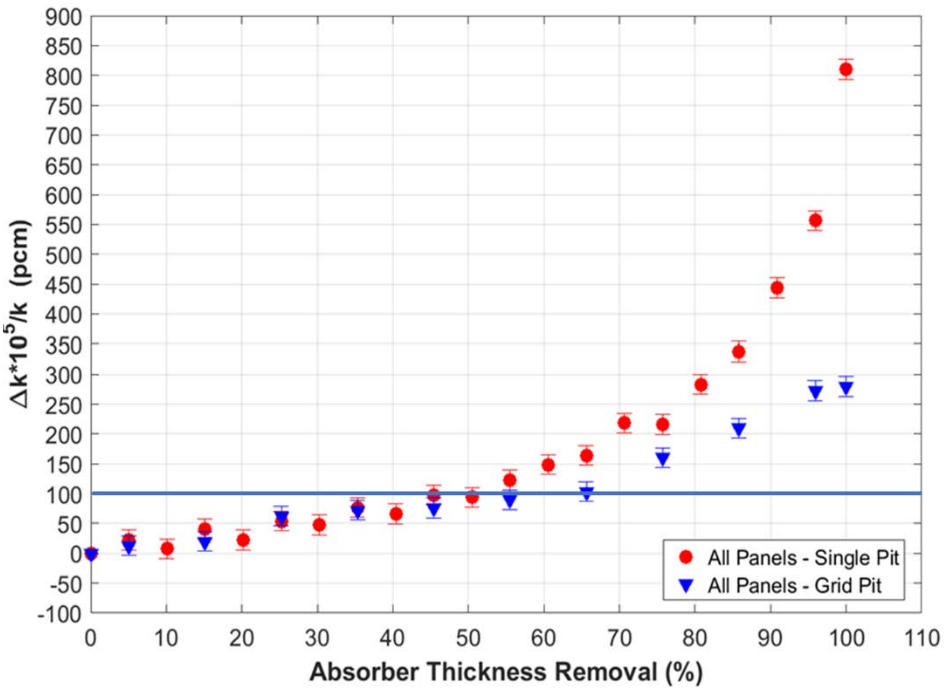

Figure 5-12
Impact of absorber thickness removal for Region 1 panels for the distributed profile

The pit worth as a function of neutron absorber panel thickness removal for Region 2 distributed profile for W17x17 fuel with 3.5 wt. % enrichment, 40 GWd/MTU burnup, and 0.015 $g^{10}B/cm^2$ areal density is presented in Figure 5-13. In this case, the pit radius for a single pit, assumed on all panels surrounding the storage cell at the same axial height, is 1.8 cm. The single pit on all panels compared against 6x10 grid pitting on all panels, at the same axial location, yields a similar area. In this case, pits are still clustered around the maximum impact location with a very fine grid. Subsequently, the impact between a single pit on all panels and grid pitting is lower. Pit worth of 100 pcm is reached when about ~85% of the thickness is removed for a single pit on all panels. For grid pitting, even when 100% is removed, the impact is below 100 pcm, as shown in the figure.

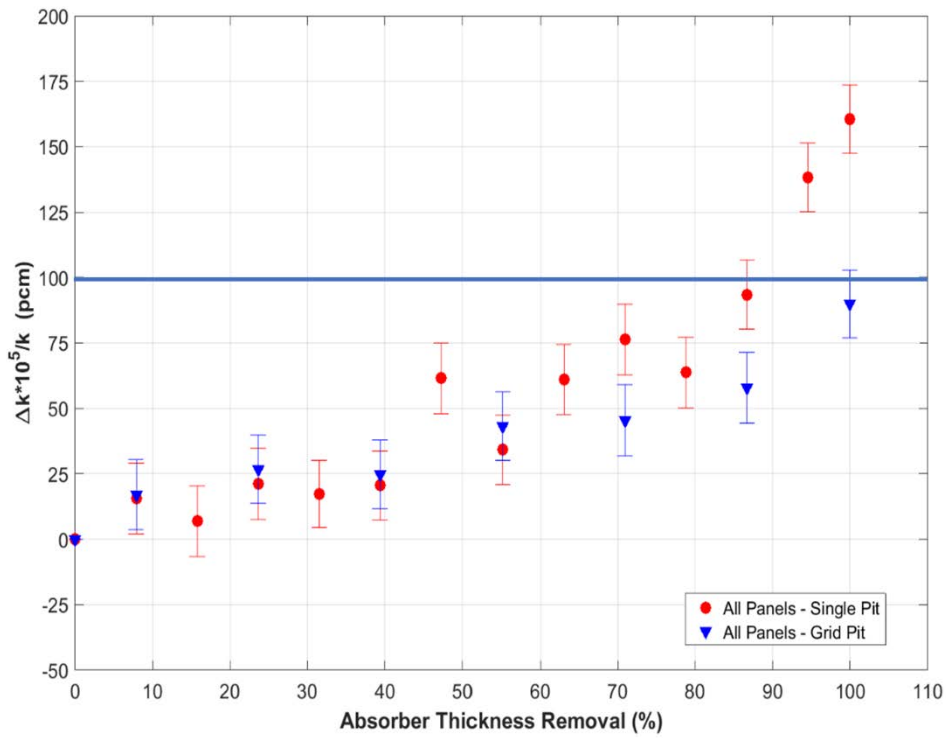

Figure 5-13
Impact of absorber thickness removal for Region 2 panels using distributed profile

Multiple pit models of similar area to the single pit remain similar at low reactivity worth, and significantly depart as the thickness of the pit approaches the panel thickness. This is primarily due to the single large pit creating a single large pathway for streaming as opposed to multiple smaller pathways where a neutron may more easily encounter absorber material. Additionally, as the area containing the multiple grid pit expands, smaller pits will extend to less neutronically important regions of the fuel assembly.

Based on the results presented in all the cases, the worth of a single pit in a single panel is substantially lower compared to all panels. Moreover, distribution of pits in a grid structure, as opposed to large pits aligned at the same axial height, reduces the impact on reactivity even for the same area of pits. The reduction depends on the distribution of the pits. This is primarily due to the single large pit creating a single large pathway for neutron streaming as opposed to multiple smaller pathways where a neutron may more easily encounter absorber material. Additionally, as the area containing the multiple grid pit expands, smaller pits will extend to less neutronically important regions of the fuel assembly. Thus, for both Region 1 and Region 2, the single pit model is an extremely penalizing representation of the overall reactivity worth.

5.7 Pitting Analysis Summary

This section has described the analysis which has been performed to determine the reactivity impact of pitting in metallic neutron absorber panels with a B_4C and Al composite. Specifically, the study focused on the reactivity impact of pitting into the neutron absorbing material itself, causing a loss of neutron absorber material and an increase in moderator. The simulations were performed for two PWR fuel types and determined that Westinghouse W17x17 fuel is bounding and applicable to all other PWR fuels. Furthermore, to keep the study as generic as possible, the simulations were performed at unborated conditions. Therefore, results are applicable to BWR SFPs.

The analyses performed to evaluate the impact of single and multiple pits at various depths with a combination of fresh fuel and depleted fuel with both uniform and distributed axial burnup profiles at three different enrichments and several burnup levels to represent both lightly and heavily depleted fuel. The results of the analyses have shown that the impact of pitting on neutron absorber panel performance is statistically insignificant for the pitting that has been identified through operating experience outlined in Reference [3].

The limiting single pit case (the case that requires the smallest radius for 100 pcm impact) is the 5.0 wt. %, 60 GWd/MTU, distributed profile case. This case requires a 1.8 cm radius pit on all panel at the exact same axial height with a depth of 0.1016 cm to cause an approximately 100 pcm reactivity impact. A pit of this size and depth removes more than 1.03 cm^3 of neutron absorber material, compared to the 0.03 cm^3 of material (panel cladding and neutron absorber) removed from the pits with the combined deepest and largest surface area (depth of 0.1016 cm and area of 0.2968 cm^2). This modeling assumption utilizes the combination of the largest radius pit with the deepest depth pit ever observed in industry (creating an artificial pit with a larger volume than ever actually observed). However, as discussed in Section 2, based on operational experience [3] and Zion coupon and panel results [4-5], this is not the case. The multiple pit studies also show that for the distributed profile cases, including the limiting case, the reactivity impact of pits is greatly reduced when multiple pits are modeled as grid pits instead of large pits which aggregates the streaming path.

The reactivity impact of pits is further reduced when only pits on a single panel are considered. The simulations that contained pits on every panel used a simplified pitting model where the pits were placed identically on each panel. This modeling simplification is very extreme and significantly overestimates the impact on reactivity as it creates enhanced neutron streaming. The single panel analysis documented in Section 5.3 shows that the impact of pitting decreases significantly when pits are not aligned.

Simulations performed using the distributed profile have been shown to be more limiting. This is mainly due to the distributed profile used in this study since it causes the reactivity of the assembly to be dependent on a relatively small axial region. In such cases, changes in the high importance axial regions will have a larger impact than in cases where the relative importance of each region is more uniform.

Section 6: Blister Modeling and Analysis

This section describes the modeling and analysis performed to determine blister reactivity worth, and ultimately, the impact on SFP criticality. The following methodology was followed to model and to assess the blister impact.

6.1 Blister Modeling

There are two major types of blister geometries used in the blister analysis, cylindrical blisters and rectangular blisters. As discussed in Section 4.5 the cylindrical blister model is defined by the blister radius and height, and the rectangular blister model is defined by the blister length, width, and height. For both cylindrical and rectangular blisters, the blister itself is modeled as a void which starts from the surface of the neutron absorber panel. The blister displaces the moderator which is nominally next to the panel. Note that the analysis in this study assumes unborated water; hence, it overestimates the criticality impact as including soluble boron will slightly reduce the impact of blisters. Figure 6-1 shows a simplified diagram of a single blister. Figure 6-2 shows a cylindrical blister of the maximum height analyzed (0.4445 cm) on a Region 1 storage cell from various views.

The blister analysis described in this section includes blister heights which extend into and beyond the stainless steel encapsulation, which holds the neutron absorber panel in place. This is a highly unlikely scenario that has never been observed to date in industry – all blisters that contact the encapsulation tend to flatten and do not result in dimensional changes to the stainless steel encapsulation. To make sure that changes in the stainless steel encapsulation do not impact the results of the blister analysis, the encapsulation has been excluded from all simulations performed with blisters. The presence of the encapsulation does change the reactivity of the simulations; however, it does not impact the change in reactivity when comparing blister cases to the base case. Therefore, the presence or lack of stainless steel encapsulation in the model does not change the overall conclusions of the study.

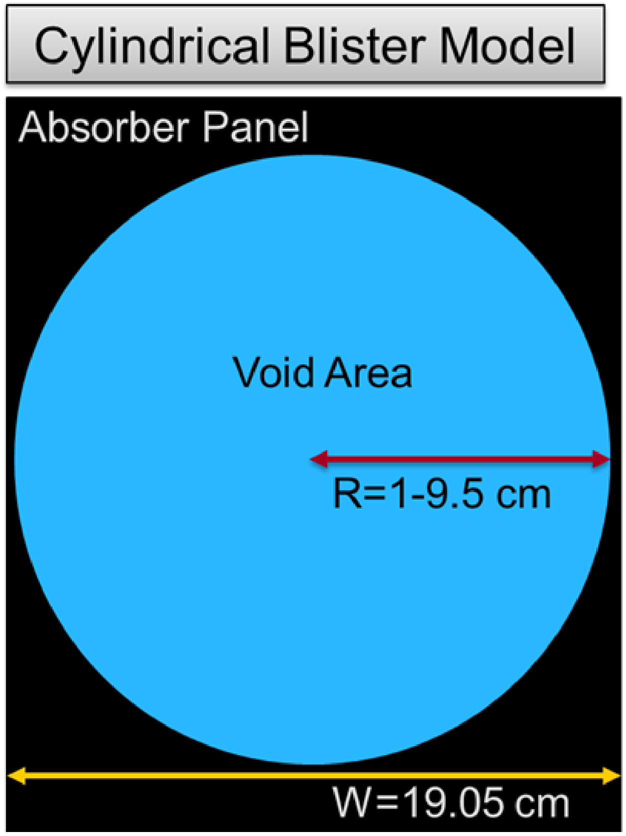

Figure 6-1
Simplified cylindrical blister for Region 1 and Region 2

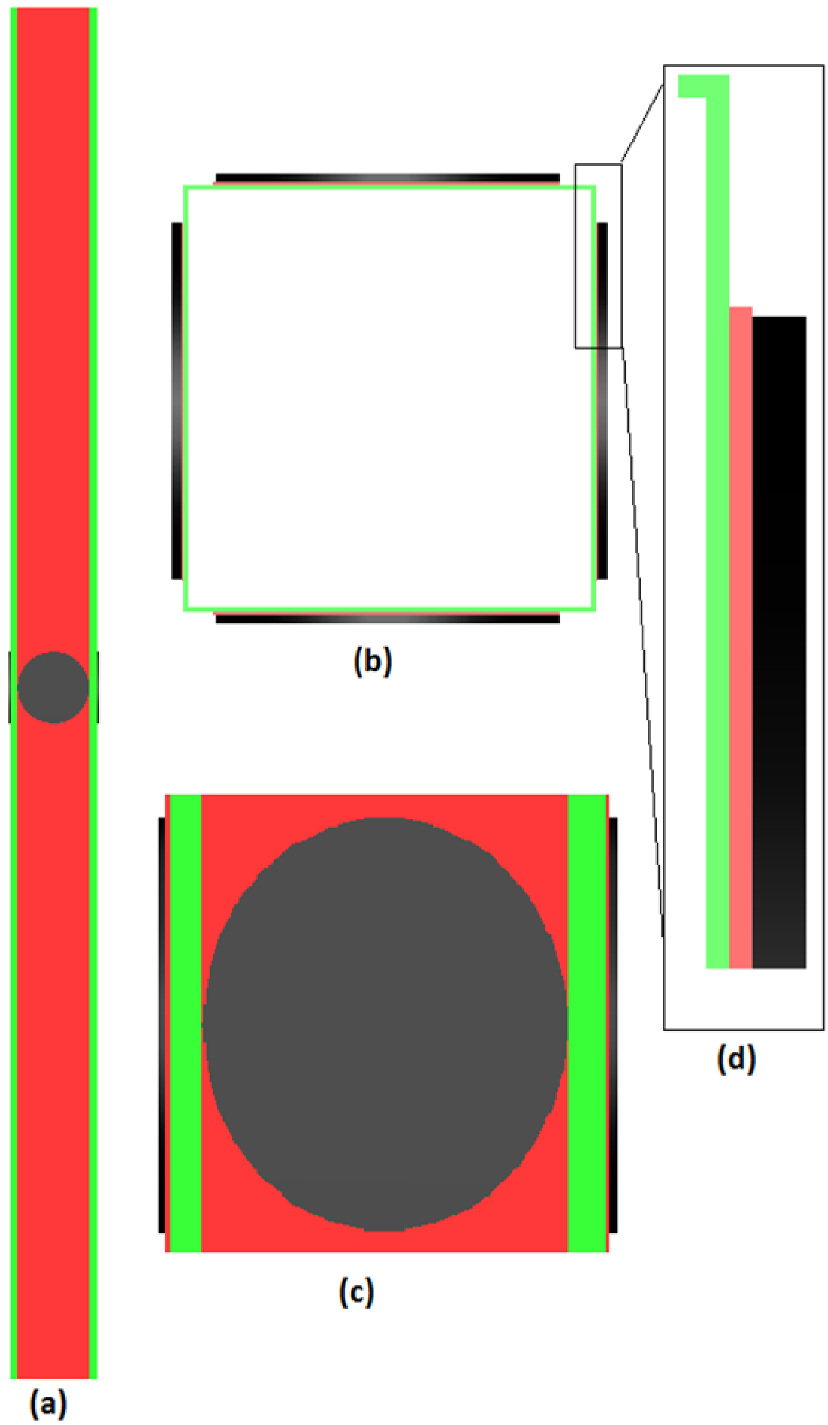

Figure 6-2
Region 1 W17x17 Keno-V.a Rack Model with a 9.5 cm Radius Blister Exposed. Red indicates neutron absorber material, black is void, and green represents stainless steel. (a) Side-view of full storage cell, (b) top view of storage cell, (c) closeup of blister from (a), and (d) magnification of storage cell wall, neutron absorber panel, and blister from (b)

6.2 Blister Analysis

Blister analysis is performed using both cylindrical and rectangular blisters. The cylindrical blister analyses are performed first to identify the reactivity impact of blisters of a variety of sizes and heights.

Following the cylindrical blister analysis, additional analyses are performed using rectangular blisters. The cylindrical blisters are limited to a maximum area based on a radius which covers the width of the panel. Therefore, rectangular blisters are used to perform simulations corresponding to very large area blisters.

6.2.1 Cylindrical Blister Analysis

The blister analysis starts with the modeling of cylindrical blisters to determine the reactivity impact of a single blister across a range of radii and heights. Blister radii of 1, 5, 7, and 9.5 cm are simulated at varying blister heights for varying enrichments, burnups (using both uniform and distributed axial burnup profiles), and absorber areal density combinations. The most limiting results (maximum blister worth) from all combinations of fuel design, areal density, enrichment and burnup are provided in Table 6-1 for Region 1. The results are based on blisters being present on all panels surrounding the storage cell, aligned at the same axial height (height corresponding to the maximum source) for both uniform and distributed profiles.

Table 6-1
Region 1 single blister on all panels for uniform and distributed profiles

Blister Height [cm]	Impact of 1.0 cm Radius [pcm]	Impact of 5.0 cm Radius [pcm]	Impact of 7.0 cm Radius [pcm]	Impact of 9.5 cm Radius [pcm]
Uniform Profile				
0.03	22.25	32.09	35.24	43.72
0.15	60.07	58.74	84.13	124.59
0.25	32.04	78.54	131.60	212.58
0.35	28.70	117.03	194.81	301.47
0.4445	24.47	110.80	230.27	422.72
Distributed Profile				
0.03	43.38	37.81	60.51	67.36
0.15	25.12	119.88	187.24	308.26
0.25	44.53	140.62	273.10	453.47
0.35	41.10	208.93	400.74	637.77
0.4445	43.73	283.14	490.94	847.15
1σ ≤ 18 pcm for all cases				

The blister cases with 9.5 cm radius and 0.4445 cm height for uniform and distributed case were further evaluated to assess the blister worth in these extreme cases in the presence of soluble boron. The uniform profile case worth was changed from 422.72 to 394.47 pcm, while the distributed profile case worth was changed from 847.15 to 881.75 pcm in the presence of soluble boron. The changes in reactivity worth for both uniform and distributed profile cases in the presence of boron are within 2σ of the original results. The results provided in Table 6-1 are shown graphically in Figure 6-3 and Figure 6-4. The figures show that the reactivity impact strongly correlates to blister radius and height.

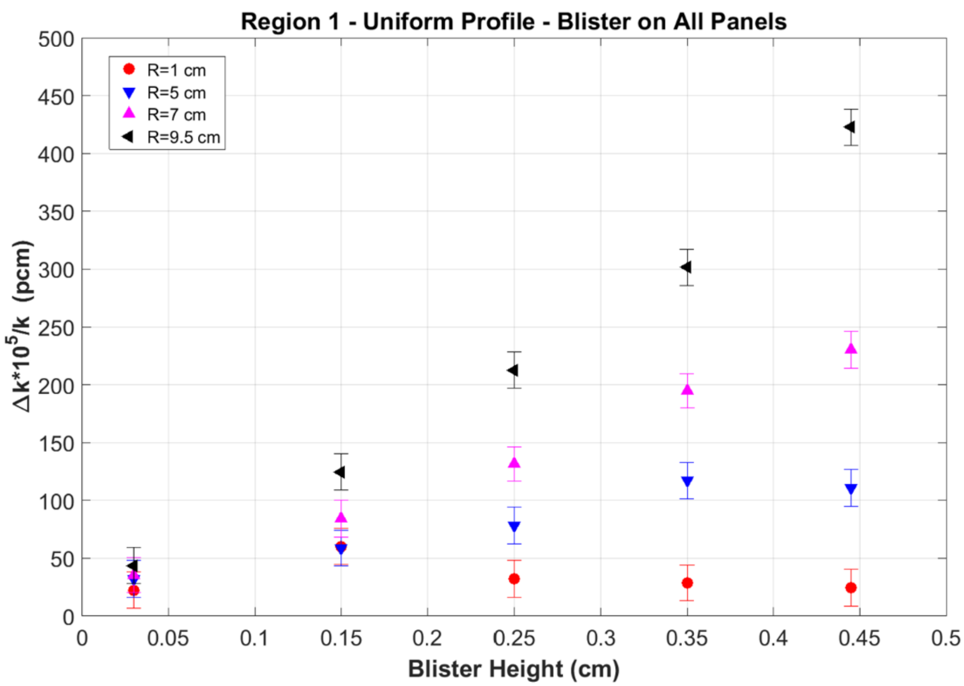

Figure 6-3
Region 1 cylindrical single blister on all panels cases - uniform profile

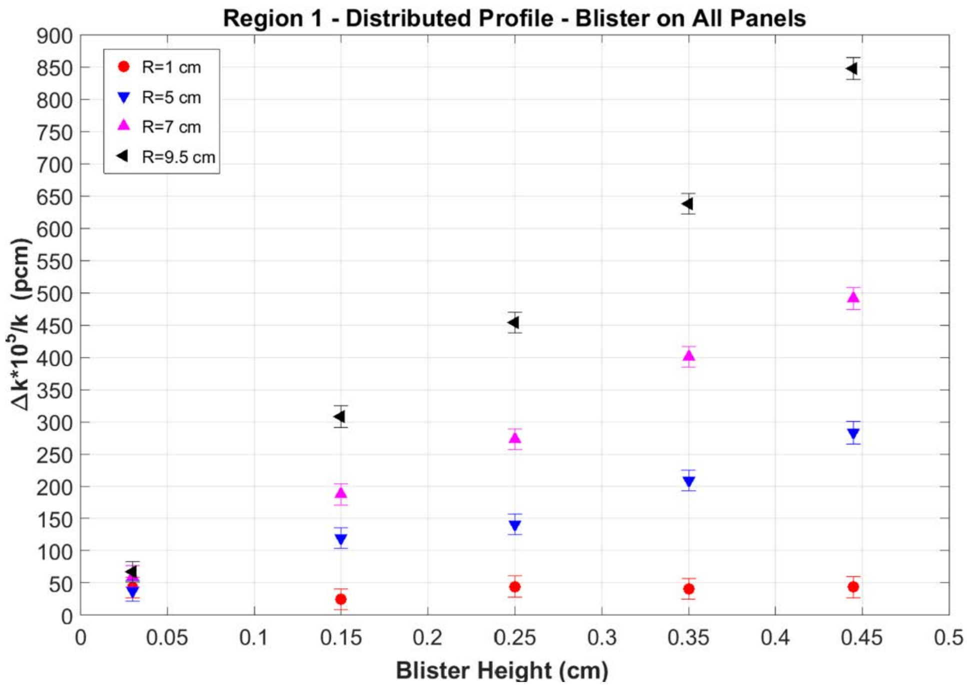

Figure 6-4
Region 1 cylindrical single blister on all panels cases - distributed profile

Additional cases were performed assuming only one panel had a blister instead of all panels surrounding the storage cell having blisters at the same exact axial height for geometric alignment. For this comparative analysis, the blister radius is assumed to be 9.5 cm. The comparison of blister on all panels versus a single panel for Region 1 using a uniform profile is presented in Figure 6-5. The same comparison using a distributed profile is presented in Figure 6-6. The values for the comparison of a single blister with radius of 9.5 cm on all panels versus on a single panel for the uniform and distributed profiles are also tabulated in Table 6-2. As is evident from the results presented in the figures and table, a blister on a single panel (or on differing areas of multiple panels) has a significantly smaller reactivity impact than the cases with blisters or pits perfectly aligned on all panels.

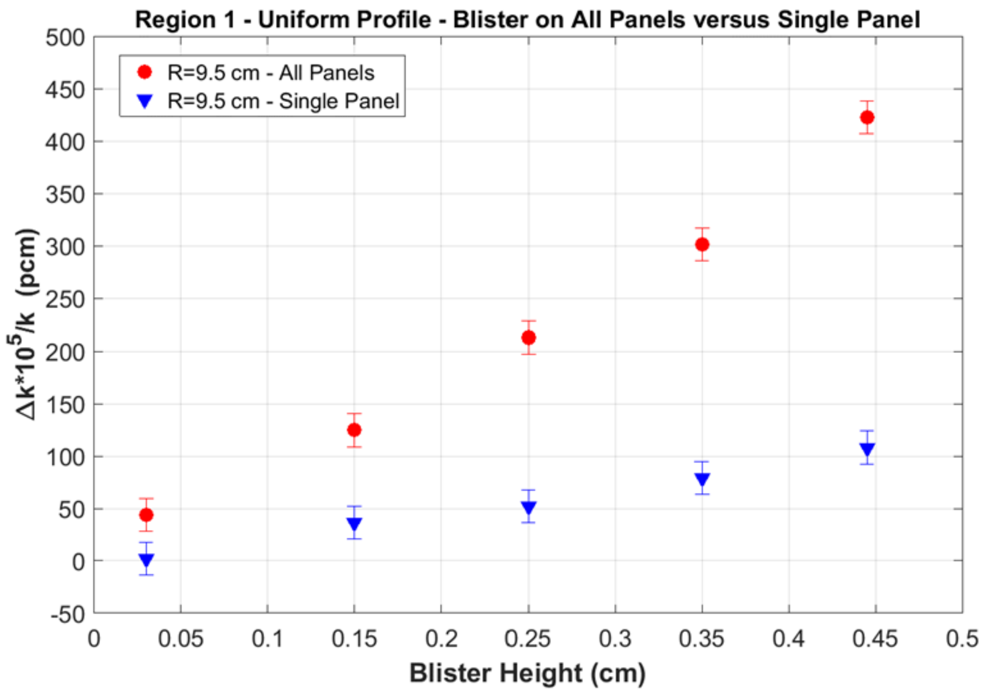

Figure 6-5
Region 1 single versus all panel cylindrical blister impact - uniform profile

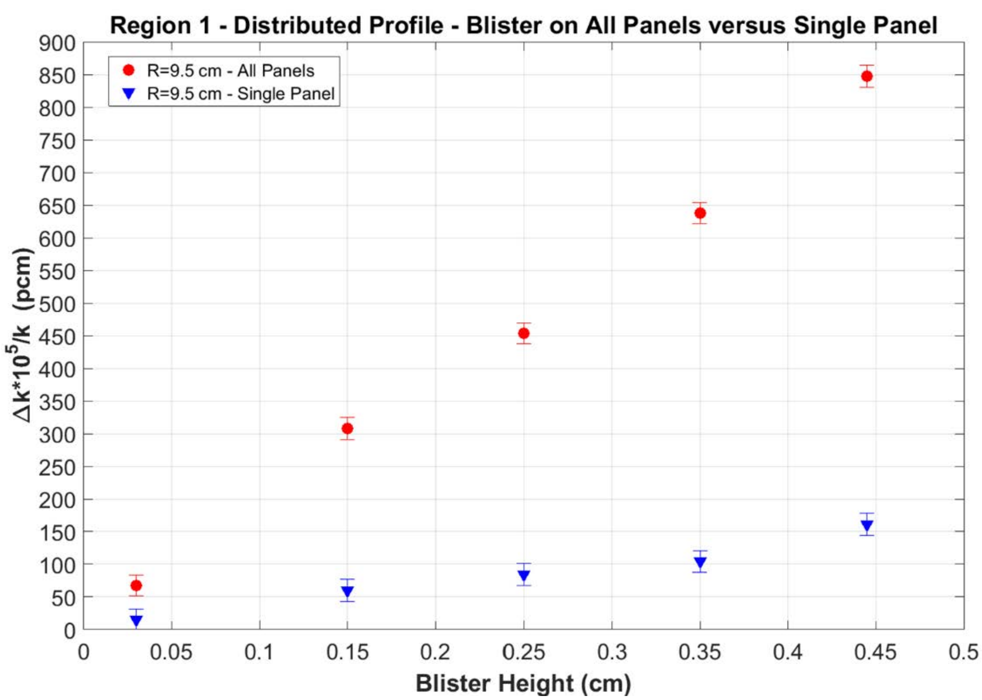

Figure 6-6
Region 1 single versus all panel cylindrical blister impact - distributed profile

Table 6-2
Region 1 single blister on all panels versus single panel for blister radius of 9.5 cm for uniform and distributed profiles

Blister Height [cm]	Uniform Profile		Distributed Profile	
	All Panels [pcm]	Single Panel [pcm]	All Panels [pcm]	Single Panel [pcm]
0.03	43.72	2.11	67.36	14.90
0.15	124.59	36.71	308.26	60.35
0.25	212.58	52.06	453.47	84.98
0.35	301.47	78.98	637.77	104.45
0.4445	422.72	108.13	847.15	161.35
1σ ≤ 18 pcm for all cases				

A similar analysis was performed for Region 2. For this region, blister radii of 1, 5, 7, and 9.5 cm are simulated at varying blister heights for varying enrichments, burnups (using both uniform and distributed axial burnup profiles), and absorber areal density combinations. The most limiting results from all combinations of fuel design, areal density, enrichment and burnup are provided in Table 6-3. The results are based on blisters being present on all panels, aligned at the same axial height (height corresponding to the maximum source) for both uniform and distributed profiles.

The blister results for Region 2 show that blisters, even with extreme sizes and heights, have little impact on reactivity in Region 2. Figure 6-7 and Figure 6-8 graphically represent the reactivity impact of blisters as a function of blister radius and height for uniform and distributed profiles for Region 2, respectively.

Table 6-3
Region 2 single blister on all panels for uniform and distributed profiles

Blister Height [cm]	Impact of 1.0 cm Radius [pcm]	Impact of 5.0 cm Radius [pcm]	Impact of 7.0 cm Radius [pcm]	Impact of 9.5 cm Radius [pcm]
Uniform				
0.03	27.01	28.45	25.40	19.93
0.15	31.74	35.09	28.99	34.75
0.25	24.79	26.44	39.53	38.62
0.35	24.64	45.10	36.01	46.94
0.4445	30.67	45.11	34.13	48.43
Distributed				
0.03	27.33	30.73	41.06	35.49
0.15	39.12	32.35	47.22	67.57
0.25	37.54	39.23	60.48	82.41
0.35	34.11	45.77	72.81	108.57
0.4445	26.80	49.45	84.86	123.07
1σ ≤ 15 pcm for all cases				

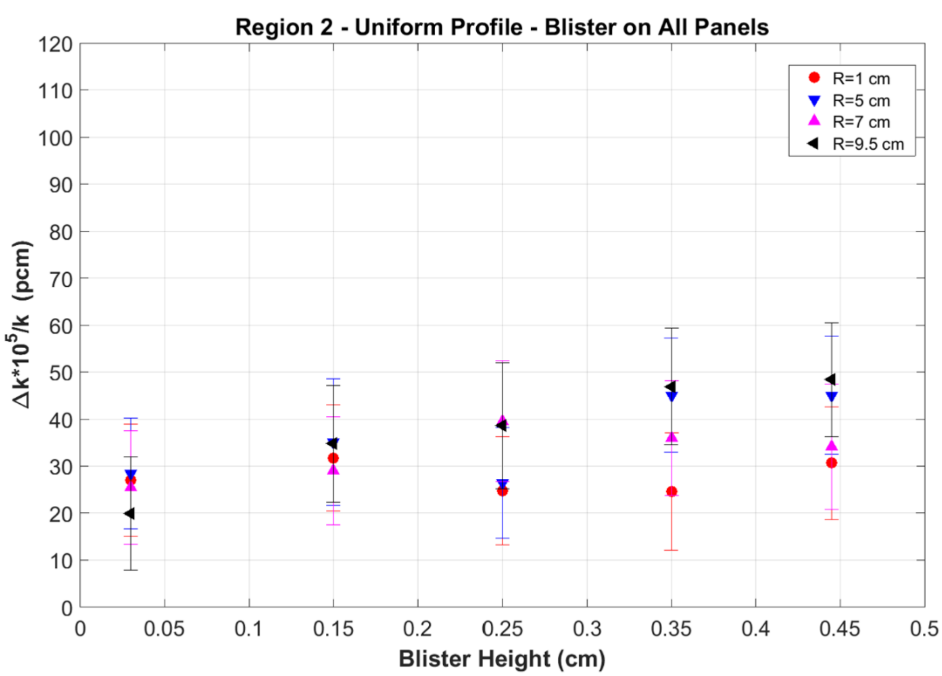

Figure 6-7
Region 2 cylindrical blister impact - uniform profile

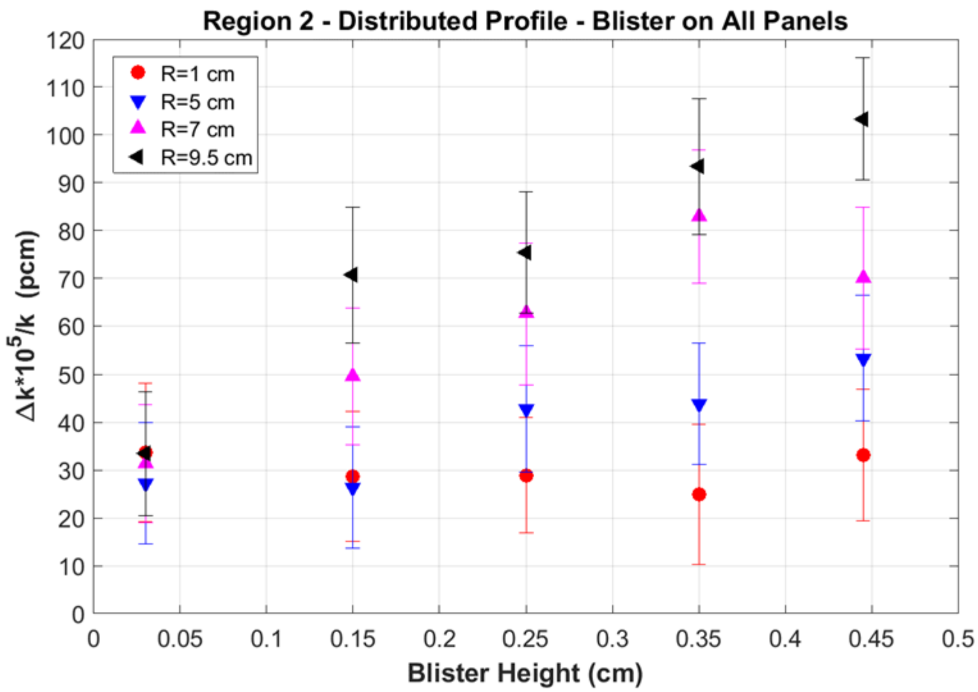

Figure 6-8
Region 2 cylindrical blister impact - distributed profile

The results presented in Figure 6-3 through Figure 6-6 illustrate the strong relationship between blister radius and reactivity for Region 1. For Region 2, there is no significant impact on reactivity independent of the radius or height of the blister as illustrated in Figure 6-7 and Figure 6-8.

One key result to note is that for both Region 1 and Region 2, there is no significant reactivity impact for cases where the blister height is constrained by the stainless steel encapsulation, which fix the panels to the rack. Therefore, for either Region 1 or Region 2, if a single blister height on a single panel is constrained by the stainless steel encapsulation and less than 9.5 cm in radius, the reactivity effect is insignificant (<100 pcm) and will not impact the results and conclusions of the underlying spent fuel pool criticality analysis.

6.2.2 Rectangular Blister Analysis

The analysis has used cylindrical blisters at the center of the panels; however, blisters have more typically formed along the edges of the panels. The reactivity impact of blisters forming along the edges of the panels would not be captured using cylindrical blisters at the center; therefore, rectangular blisters have also been analyzed. The rectangular blisters cover the full width of the panel and three axial lengths, 7.62 cm, 15.24 cm, and 30.48 cm (3, 6, and 12 inches) at a blister height of 0.4445 cm (0.175 in.).

Table 6-4 contains the final results for the maximum impact case perturbations. While these results indicate that there can be a significant reactivity impact in

Region 1 for blistering, only for the cases at the maximum blister height of 0.4445 cm for large blister radii, which is significantly beyond operating experience to date. For the 0.03 cm blister height cases, which corresponds to approximately the gap between the neutron absorber panel and the stainless steel encapsulation, the reactivity impacts of blisters are generally statistically insignificant and even where they are statistically significant they remain small (~100 pcm) and would not invalidate the results and conclusions of either spent fuel pool storage specifications or the supporting criticality analysis.

It is worth noting that the volumes of individual blisters for the three cases in Table 6-3 are 64.52, 129.05, and 258.096 cm^3. The reactivity impacts of the rectangular blister cases to the equivalent volume results given in Figure 6-9 and Figure 6-10 show that the cylindrical blister results are more conservative than the rectangular blisters of the same volume.

Table 6-4
Region 1 limiting rectangular blisters, W17x17, 5 wt. %, 0.015 $g^{10}B/cm^2$

W17x17 5 wt%, 0.015 $g^{10}B/cm^2$ (All panels)	Fresh	10 GWd/MTU Uniform	10 GWd/MTU Distributed
Axial Length	**pcm[2]**		
0.03 cm Height (Operating experience)			
Middle 7.62 cm (3 in.)	-15.54	-2.67	-19.68
Middle 15.24 cm (6 in.)	5.18	-13.35	-6.41
Middle 30.48 cm (12 in.)	15.54	22.24	2.43
7.62 cm (3 in.) Zone 16[1]	-8.29	-2.67	21.45
15.24 cm (6 in.) Zone 16[1]	3.11	-25.58	42.23
30.48 cm (12 in.) Zone 16[1]	-5.18	-14.46	80.92
0.4445 cm Height (Extreme case scenario)			
Middle 7.62 cm (3 in.)	152.33	164.64	6.85
Middle 15.24 cm (6 in.)	394.80	385.34	1.33
Middle 30.48 cm (12 in.)	877.68	873.25	0.66
7.62 cm (3 in.) Zone 16[1]	35.23	48.95	380.62
15.24 cm (6 in.) Zone 16[1]	149.22	135.72	787.32
30.48 cm (12 in.) Zone 16[1]	503.61	491.69	1612.00
Notes: 1. 314.96 cm (124 in.) axial height 2. 1σ standard deviation is between 14 and 16 pcm (all cases)			

Data in Table 6-5 show that even for the enlarged blisters, there is minimal reactivity impact associated with blisters in Region 2. For both Region 1 and Region 2, when comparing the cylindrical blisters against rectangular blisters of the same volume, the rectangular blisters cause a lower reactivity effect. Therefore, it can be concluded that blisters along the edge of the panels are neutronically less important than the blisters in the middle (radial not vertical) of the panel.

Additional cases have been performed to provide insight into purely hypothetical blisters which cover at least one third of each neutron absorber panel. Cases are performed assuming blisters that cover one-third, two-thirds, or the entire panel at a blister height of 0.4445 cm. Additional cases are performed using a height of 0.03 cm to provide information on the impact of those extreme blister sizes when the blister height is constrained by the stainless steel encapsulation.

Table 6-5
Region 2 limiting rectangular blisters, CE16x16, 5 wt. %, 0.015 g^{10}B/cm^2

CE16x16, 5 wt. %, 0.015 g^{10}B/cm^2 (All Panels)	Fresh Fuel	10 GWd/MTU (Uniform)	10 GWd/MTU (Distributed)
Axial Length	**pcm(2)**		
0.03 cm Height			
Full Panel	18.42	40.06	13.94
0.4445 cm Height			
Middle 15.24 cm (6 in.)	31.28	35.09	-15.02
Middle 30.48 cm (12 in.)	52.65	74.07	11.42
Middle 38.10 cm (15 in.)	90.91	81.03	7.82
Middle 45.72 cm (18 in.)	111.51	126.16	19.15
Middle 60.96 cm (24 in.)	149.61	149.04	-2.97
15.24 cm (6 in.) Zone 17(1)	4.46	4.88	78.78
30.48 cm (12 in.) Zone 17(1)	7.32	2.35	169.15
38.10 cm (15 in.) Zone 17(1)	6.90	18.81	221.85
45.72 cm (18 in.) Zone 17(1)	5.30	30.66	270.41
60.96 cm (24 in.) Zone 17(1)	29.94	34.73	323.47
Top 121.92 cm (48 in.)	112.35	144.61	404.49
Top 243.84 cm (96 in.)	414.52	413.75	419.51
Full Panel	486.25	463.67	428.95

Notes:
1. 337.82 cm (133 in.) axial height
2. 1σ standard deviation is between 11 and 13 pcm all (cases)

Table 6-6 shows the results of these extreme blistering cases. While blistering has a large reactivity impact when covering at least one-third of the panel at a height of 0.4445 cm, the effect is significantly reduced when a blister height of 0.03 cm is used in the simulation. This shows that when a blister is constrained by the stainless steel encapsulation, there is only a small reactivity impact under even extreme conditions.

Table 6-7 repeats the full panel cases from Table 6-6 using an areal density of 0.030 $g^{10}B/cm^2$ showing that at a higher areal density the impact of the blister was somewhat smaller.

Table 6-6
Region 1 extreme cases: W17x17, 5 wt. %, all panels 0.015 $g^{10}B/cm^2$

Case	Fresh	10 GWd/MTU Uniform	10 GWd/MTU Distributed
Axial Length	**pcm[1]**		
0.03 cm Blister Height			
Middle 121.92 cm (48 in.)	130.53	126.78	-4.75
Middle 243.84 cm (96 in.)	164.71	190.17	57.37
Top 121.92 cm (48 in.)	14.50	7.79	219.77
Full Panel	186.47	202.40	204.96
0.4445 cm Blister Height			
Middle 121.92 cm (48 in.)	2804.03	2849.24	807.66
Middle 243.84 cm (96 in.)	3452.71	3480.77	1982.78
Top 121.92 cm (48 in.)	2510.78	2520.75	3439.47
Full Panel	3593.63	3605.36	3469.98
Notes: 1. 1σ standard deviation is between 14 and 16 pcm (all cases)			

Table 6-7
Region 1 extreme cases: W17x17, 5 wt. %, all panels 0.030 $g^{10}B/cm^2$

Case	Fresh	10 GWd/MTU Uniform	10 GWd/MTU Distributed
Axial Length	**pcm[(1)]**		
<u>0.03 cm Blister Height</u>			
Full Panel	222.33	199.89	221.38
<u>0.4445 cm Blister Height</u>			
Full Panel	3426.38	3456.35	3366.18
Notes: 1. 1σ standard deviation is between 15 and 17 pcm (all cases)			

6.3 Blister Analysis Results and Conclusions

The blister analysis evaluated the reactivity impact of both cylindrical shaped blisters starting in the radial center of the panel and rectangular 'strips' of blisters going from one panel edge to the other for various heights. These analyses have included simulations incorporating blisters significantly larger than have been seen in operating experience. There are several important conclusions that can be derived from these results.

- The reactivity impact of blistering is a strong function of blister height and radius, primarily in Region 1.
- Blisters along the edges of panels have a lower reactivity impact than blisters that form in the radial middle of the panel.
- For Region 1 racks, blister sizes observed to date, based on operational experience do not significantly impact system reactivity.
- For Region 1 racks, some extreme cases are modeled, in these cases if the blister extends beyond the encapsulation or along the entire panel, it has a non-negligible impact on reactivity, assuming all panels surrounding the storage cell have such large blisters at the same axial height. This impact is significantly reduced when blister growth is limited to one panel and becomes insignificant. The potential for blister growth on all panels at the exact same height, symmetrically at the same size, is highly unlikely.
- For Region 2 racks, blisters do not impact system reactivity such that the results and conclusions of criticality analyses or the technical specifications the analyses support would be invalidated (see Table 6-5).

Section 7: Results and Conclusions

The impact of blisters and pits on the SFP reactivity for metallic neutron absorber materials that contain B_4C and Al has been evaluated and presented in this report. This section summarizes the analyses discussed in the previous sections and utilizes those analyses to identify the area(s) of applicability, and develops conclusions on the reactivity impacts of blisters and pits.

Blister and pit simulations have been performed to cover conditions ranging from essentially pristine neutron absorber panels to panels with defects which go far beyond current operating experience. As outlined in previous sections, this report covers:

- Multiple burnup and enrichment combinations
- Axially distributed and uniform burnup profiles
- Single pits at a variety of radii, depths, and axial locations
- Matrices of pits at a variety of radii, depths, and axial locations
- Single blisters at a variety of radii, heights, and axial locations
- Partial panel blisters at a variety of sizes and axial locations at the maximum blister height seen to date, based on operating experience
- Full panel-length blisters

Covering this range of conditions provides an understanding of how the condition of neutron absorber panels present in spent fuel pools will impact the results and conclusions of the criticality safety analyses performed to support safe operation which is not dependent on remaining within the current operating experience.

7.1 Pit Results and Conclusions

Based on the analysis performed, pitting on the metallic neutron absorber panels containing B_4C and Al will not provide an impact to system reactivity that would require the results and conclusions of a spent fuel pool criticality analysis to be revisited unless an area of approximately 30 cm by 20 cm shows greater than 10 cm^2 of pitting that removes over half of the neutron absorber material. Even if such a level of pitting were to occur, it may still result in an insignificant reactivity increase (<100 pcm) since the evaluation methods in this report utilized several assumptions, including pitting on all panels at the exact same axial height surrounding the storage cell, that bias the results towards artificially higher pitting worth.

7.2 Blister Results and Conclusions

Based on the analysis performed, blistering on the neutron absorber materials observed to date has negligible impact on system reactivity. For Region 1 rack designs, the operating experience to date results in insignificant impact on reactivity and significant margins exist before any impact would be observed. However, in the unlikely case of formation of large scale blisters that could cause bulging on all panels surrounding the storage cell simultaneously, there is a potential for reactivity impact. The probability of all panels surrounding the storage cells distorting the stainless steel encapsulation simultaneously is extremely small.

Based on the computational results, for Region 2 rack designs, the impact of blisters on reactivity is insignificant even when there are large blisters on all panels surrounding the storage cell at the same axial height.

The study results demonstrate that pitting and blistering, on a scale much larger than any that has been observed in the industry operating experience to date, still has an insignificant impact on SFP criticality.

7.3 Comparison to Operating Experience

The work documented in this report reviewed operating experience and performed blistering and pitting simulations to identify blister and pit scenarios where there could be a reactivity effect that require the re-evaluation of the SFP criticality analysis. To obtain such reactivity impacts, the models developed for both blistering and pitting had to make assumptions that are far beyond what has been seen through operating experience to-date. This is beneficial because it:

1. shows that the blistering and pitting phenomena seen in operating experience until the publication of this report have negligible impact on system reactivity, and
2. allows the report to be used as the technical basis for quantifying the reactivity impact of future operating experience even if it significantly exceeds current operating experience.

The blistering and pitting data from operating experience were presented and compared to simulation results. The results show that the blistering and pitting observed based on the operating experience to date have an insignificant impact on SFP criticality, even when the impact of blisters and pits are combined. Furthermore, for any statistically significant impact on reactivity, significant margins beyond operating experience to date exist. Continued monitoring and participation in the industrywide monitoring program [13] are recommended to ensure potential issues are identified early and confirm safety margins are maintained.

7.4 Area of Applicability

The results and conclusions presented in this report are applicable to wet storage environments using all metallic neutron absorber materials containing B_4C and Al for all PWR and BWR SFPs. The simulations were performed for two fuel types, varying enrichment, burnup, and neutron absorber areal density values at unborated conditions to ensure applicability for BWR fuel. The results demonstrate that independent of the fuel type, enrichment, and burnup, the blister and pit sizes are the driving force for potential reactivity impact.

The operating experience discussed in this report is based on the BORAL® neutron absorber material. Due to different manufacturing methods including any heat-treatment, rolling, encapsulation, etc., neutron absorber panel performance in the spent fuel pool may vary. However, from a simulation perspective, the neutron absorber panel manufacturer does not impact the panel's reactivity hold-down. Rather, so long as the blister or pit is within the bounds covered in this report, the results and conclusions on reactivity impact remain valid regardless of the manufacturer or type of the neutron absorber panel, provided the metallic neutron absorber is a composite of B_4C and Al.

Additionally, the results presented in this report demonstrate that the reactivity impact of both blisters and pits is based upon the geometry of the blister or pit rather than the material providing the neutrons (the fuel stored in the rack). While BWR fuel was not explicitly simulated, the simulations were performed at unborated conditions. Furthermore, there are several aspects of BWR fuel that would make it bounded by PWR fuel. First, BWR fuel contains more neutron absorbers (gadolinia). Second, BWR storage cells are smaller than PWR storage cells. At the point of peak reactivity for a BWR (the assumed time of storage), there is still a significant amount of burnable absorber in the fuel assembly which will compete with and therefore lower the worth of the neutron absorber panel.

Therefore, the results and conclusions presented in this report are applicable to identifying the reactivity impacts of blisters and pits for all metallic neutron absorber materials containing B_4C and Al for all BWR and PWR fuels and SFPs.

Section 8: References

1. *Handbook of Neutron Absorber Materials for Spent Nuclear Fuel Transportation and Storage Applications: 2009 Edition*. EPRI, Palo Alto, CA: 2009. 1019110.
2. M. L. Eyre *et al*., "MAXUS® Corrosion Performance in Spent Fuel Pool Environments After 3 Years of 5-Year Accelerated Corrosion Testing", *Proceedings of the 18th International Symposium on the Packaging and Transportation of Radioactive Materials*, PATRAM 2016, September 2016.
3. *Overview of BORAL® Performance Based Upon Surveillance Coupon Measurements*. EPRI, Palo Alto, CA: 2010. 1021052.
4. *Evaluation of BORAL® Coupons from Zion Spent Fuel Pool*. EPRI, Palo Alto, CA: 2016. 3002008195.
5. *Evaluation of BORAL® Panels from Zion Spent Fuel Pool and Comparison to Zion Coupon*s. EPRI, Palo Alto, CA: 2016. 3002008196.
6. H. Akkurt, S. Feuerstein, M. Harris, and S. Baker, "Overview of Zion Comparative Analysis Project for Assessment of BORAL® Neutron Absorber Material Performance and Monitoring in Spent Fuel Pools," *Proceedings of the ANS Conference: 2015 International Conference on Nuclear Criticality Safety*. Charlotte, NC (September 13–17, 2015).
7. H. Akkurt, S. Feuerstein, M. Harris, and A. Quigley, "Analysis of BORAL® Coupons from Zion Spent Fuel Pool," *Trans. Am. Nuc. Soc.*, 113, 372–375 (2015).
8. H. Akkurt, M. Harris, A. Quigley, "Evaluation of Neutron Absorber Panels from Zion Spent Fuel Pool," *Trans. Am. Nuc. Soc.*, 115, 645–647 (2016).
9. H. Akkurt, "Comparison of Neutron Absorber Panels and Monitoring Coupons from Zion Spent Fuel Pool," *Proc. of International High-Level Radioactive Waste Management (IHLRWM 2017)*, April 2017, Charlotte, NC.
10. H. Akkurt, A. Quigley, M. Harris, "Accelerated Corrosion Tests to Evaluate Long-Term Performance of BORAL® in Spent Fuel Pools," *Trans. Am. Nuc. Soc.*, 115, 306-309, (2016).
11. H. Akkurt, A. Quigley, M. Harris, "Update on Accelerated Corrosion Tests for the Evaluation of Long-Term Performance of BORAL® in Spent Fuel Pools," *Trans. Am. Nuc. Soc.*, 117, 319-322, (2017).

12. H. Akkurt, A. Quigley, and M. Harris, "Accelerated Corrosion Tests for the Evaluation of Long-Term Performance of Boral in Spent Fuel Pools," *Radwaste Solutions*, V 25, No 1, 41-43, Spring 2018.
13. *Roadmap for Industrywide Learning Aging Monitoring Program (i-LAMP) For Neutron Absorber Materials in Spent Fuel Pool*s. EPRI, Palo Alto, CA: 2018. 3002013122.
14. *Sensitivity Analysis for Spent Fuel Pool Criticality – Revision 1*, EPRI, Palo Alto, CA: 2017, 30022008197.
15. Scale: A Comprehensive Modeling and Simulation Suite for Nuclear Safety Analysis and Design, ORNL/TM-2005/39, Version 6.1, June 2011. Available from Radiation Safety Information Computational Center at Oak Ridge National Laboratory as CCC-785.
16. Recommendations for Addressing Axial Burnup in PWR Burnup Credit Analyses, U.S. Nuclear Regulatory Commission, NUREG/CR-6801, March 2003.
17. NEI 12-16, Rev. 3, *Guidance for Performing Criticality Analyses of Fuel Storage at Light-Water Reactor Power Plants*, November 2017.

Program:

Used Fuel and High-Level Waste Management

3002013119

Electric Power Research Institute
3420 Hillview Avenue, Palo Alto, California 94304-1338 • PO Box 10412, Palo Alto, California 94303-0813 USA
800.313.3774 • 650.855.2121 • askepri@epri.com • www.epri.com